The American Journal of Pathology, Vol. 193, No. 1, January 2023

ELSEVIER

The American Journal of PATHOLOGY

ajp.amjpathol.org

TUMORIGENESIS AND NEOPLASTIC PROGRESSION

Overexpression of Estrogen Receptor α in Mammary Glands of Aging Mice Is Associated with a Proliferative Risk Signature and Generation of Estrogen Receptor α—Positive Mammary Adenocarcinomas

Priscilla A. Furth,*† Weisheng Wang,* Keunsoo Kang,‡ Brendan L. Rooney,* Grace Keegan,* Vinona Muralidaran,* Justin Wong,* Charles Shearer,* Xiaojun Zou,* and Jodi A. Flaws§

From the Departments of Oncology and Medicine,† Georgetown University, Washington, District of Columbia; the Department of Microbiology,‡ College of Science and Technology, Dankook University, Cheonan, Republic of Korea; and the Department of Comparative Biosciences,§ University of Illinois Urbana-Champaign, Urbana, Illinois*

Accepted for publication September 28, 2022.

Address correspondence to Priscilla A. Furth, M.D., Georgetown University, 3970 Reservoir Rd. N.W., Research Bldg., Room E407A, Washington, DC 20057.
E-mail: paf3@georgetown.edu.

Age is a risk factor for human estrogen receptor—positive breast cancer, with highest prevalence following menopause. While transcriptome risk profiling is available for human breast cancers, it is not yet developed for prognostication for primary or secondary breast cancer development utilizing at-risk breast tissue. Both estrogen receptor α (ER) and aromatase overexpression have been linked to human breast cancer. Herein, conditional genetically engineered mouse models of estrogen receptor 1 (*Esr1*) and cytochrome P450 family 19 subfamily A member 1 (*CYP19A1*) were used to show that induction of *Esr1* overexpression just before or with reproductive senescence and maintained through age 30 months resulted in significantly higher prevalence of estrogen receptor—positive adenocarcinomas than *CYP19A1* overexpression. All adenocarcinomas tested showed high percentages of ER^+ cells. Mammary cancer development was preceded by a persistent proliferative transcriptome risk signature initiated within 1 week of transgene induction that showed parallels to the Prosigna/Prediction Analysis of Microarray 50 human prognostic signature for early-stage human ER^+ breast cancer. *CYP19A1* mice also developed ER^+ mammary cancers, but histology was more divided between adenocarcinoma and adenosquamous, with one ER^- adenocarcinoma. Results demonstrate that, like humans, generation of ER^+ adenocarcinoma in mice was facilitated by aging mice past the age of reproductive senescence. *Esr1* overexpression was associated with a proliferative estrogen pathway—linked signature that preceded appearance of ER^+ mammary adenocarcinomas. *(Am J Pathol 2023, 193: 103—120; https://doi.org/10.1016/j.ajpath.2022.09.008)*

Prevalence of human estrogen receptor α (ER)—positive breast cancer increases with age following menopause.[1] Associated risk factors include estrogen exposure, either endogenous or exogenous, increased aromatase levels in the breast, and increased ER expression levels in mammary epithelial cells.[2—5]

Several gene expression—based prognostic panels are available to assist both younger and older patients with breast cancer in choosing therapeutic options, including the Prosigna/Prediction Analysis of Microarray (PAM) 50 profile targeted toward use for early-stage ER^+ breast cancer.[6,7] Eventually, transcriptome-based assays may have a role in predicting the likelihood of a primary breast cancer initiating within breast epithelium.[8—10]

Genetically engineered mouse models (GEMMs) offer the opportunity to investigate the impact of specific molecular perturbations within the context of regular lifespan events, including aging and reproductive senescence.[11,12]

Supported by NIH UH3CA213388 (P.A.F.) and NIH P30CA051008 (P.A.F.).

Disclosures: None declared.

Current address of W.W., Department of Microbiology, Immunology and Tropical Medicine, George Washington University, Washington, DC.

https://doi.org/10.1016/j.ajpath.2022.09.008

Conditionally targeted overexpression of both estrogen receptor α [estrogen receptor 1 (*Esr1*)] and aromatase [cytochrome P450 family 19 subfamily A member 1 (*CYP19A1*)] in mouse mammary epithelial cells before reproductive senescence results in generation of increased prevalence of preneoplasia and mammary cancer.[13–16] Although the prevalence of preneoplasia before reproductive senescence is high in these models, the development of adenocarcinoma is much lower, with a significant percentage of triple-negative adenocarcinomas or low percentage of ER^+ cells. One impetus for this study was to experimentally test whether postponing induction of *Esr1* and *CYP19A1* to age 12 months and then following the mice past reproductive senescence until age 30 months would result in an increased prevalence of ER^+ adenocarcinoma with high proportions of ER^+ cells, as is seen in women with aging after menopause.[1,2] A second goal of the study was to determine whether the molecular pathogenesis of mammary cancer generation in the mice paralleled human disease at the transcriptional level. Because there are relatively few studies available that focus on transcriptional risk profiles of human breast tissue before breast cancer generation, exploratory comparisons were made to a prognostic profile for early-stage ER^+ breast cancer Prosigna/PAM50.[6,8]

In women, it can be arduous to obtain breast tissue before breast cancer development. Moreover, few funding institutions can afford studies that enroll women well before breast cancer generation and follow them through aging and menopause. Cross-sectional studies are more frequent.[17] Polygenic risk score linked higher scores to higher counts of terminal duct lobular units, thought to represent anatomic structures originating breast cancer.[18] An advantage of GEMM studies is the ability to follow disease pathogenesis from early through late stages at both tissue pathology and molecular levels.[19,20]

There are challenges to aging mice through 30 months of age related to the increased rate of cohort loss that accompanies aging and the need for more intense monitoring of their health after 15 months of age.[21] Expense increases and challenges with historical data are cited as reasons for focusing studies on younger mice, even when age is a cited experimental variable.[22] Age 23 months was the oldest age studied in a study of aging mammary gland morphology focusing on a substrain of FVBN mice (FVB/N-RC).[23] A strength in planning this study included the fact that the GEMMs utilized were repeatedly studied in the context of different genetic, chemical, and therapeutic interventions over many years, providing reproducible reference data at younger ages.[13–16,24–27]

Materials and Methods

Mouse Models

The animal research protocol was approved by the Georgetown University (Washington, DC) Institutional Animal Care and Use Committee, and all regulations concerning the use of animals in research were followed in all experiments performed for this study. Mouse mammary tumor virus–reverse tetracycline–controlled transactivator/Tet-operator (tet-op)–*Esr1* and mouse mammary tumor virus–reverse tetracycline–controlled transactivator/tet-op–*CYP19A1* mice on a C57Bl/6 background were bred in the Georgetown University Department of Comparative Medicine facility and genotyped at weaning (Transnetyx, Inc., Cordova, TN). Cohorts were filled by sequentially distributing genotyped mice from different litters into the 16 cohorts studied herein. All cohorts were raised on Department of Comparative Medicine standard laboratory mouse chow until 12 months of age. Dependent on cohort assignment, mice were either maintained on Department of Comparative Medicine standard laboratory chow throughout the experiment or changed to a diet containing 200 mg doxycycline per kilogram food (Bio-Serv, Flemington, NJ) for transgene induction at age 12 or 18 months. Euthanasia was conducted according to the approved animal protocol using CO_2 inhalation followed by cervical dislocation. All mice were individually followed up for disease development or spontaneous cage death as they were aged to end points 12, 18, 24, and 30 months of age. Mice were euthanized before experimental end points, according to the approved research protocol for pain/distress/infection unresponsive to treatment, severe lethargy or weakness, severe neurologic signs, severe respiratory distress, total tumor burden >2 cm, weight loss ≥15% of body weight, or wounds refractory to treatment. Cage deaths were unpredicted spontaneous deaths lacking an identifiable cause. Initial cohort size was determined utilizing established predicted survival rates until planned end points (eg, age 12 months: 95% survival; age 18 months: 90% survival; age 24 months: 50% survival; and age 30 months: 10% survival) and designed for the numbers of mice desired at the projected end point age (age 12 months: $n = 15$; age 12.25 months: $n = 5$; age 18 months: $n = 20$; age 18.25 months: $n = 5$; age 24 months: $n = 20$; and age 30 months: $n = 15$). Numbers of mice for each genotype actually entered into each cohort with numbers retained until end point age (percentage), loss for spontaneous cage, or early necropsy are as follows: *Esr1* age 12 months entered $n = 17$, end point $n = 17$ (100%); age 12.25 months entered $n = 7$, end point $n = 6$ (86%), early necropsy $n = 1$; age 18 months entered $n = 24$, end point $n = 22$ (92%), cage death $n = 2$; age 18.25 months entered $n = 8$, end point $n = 5$ (63%), cage death $n = 2$, early necropsy $n = 1$; age 24 months no transgene induction $n = 40$, end point $n = 26$ (65%), cage death $n = 9$, early necropsy $n = 7$; age 24m with 6m transgene induction $n = 41$, end point $n = 25$ (61%), cage death $n = 11$, early necropsy $n = 5$; age 24m with 12m transgene induction $n = 50$, end point $n = 25$ (50%), cage death $n = 12$, early necropsy $n = 13$; age 30m with 18m transgene induction entered $n = 126$, end point $n = 18$ (14%), cage death $n = 54$, early

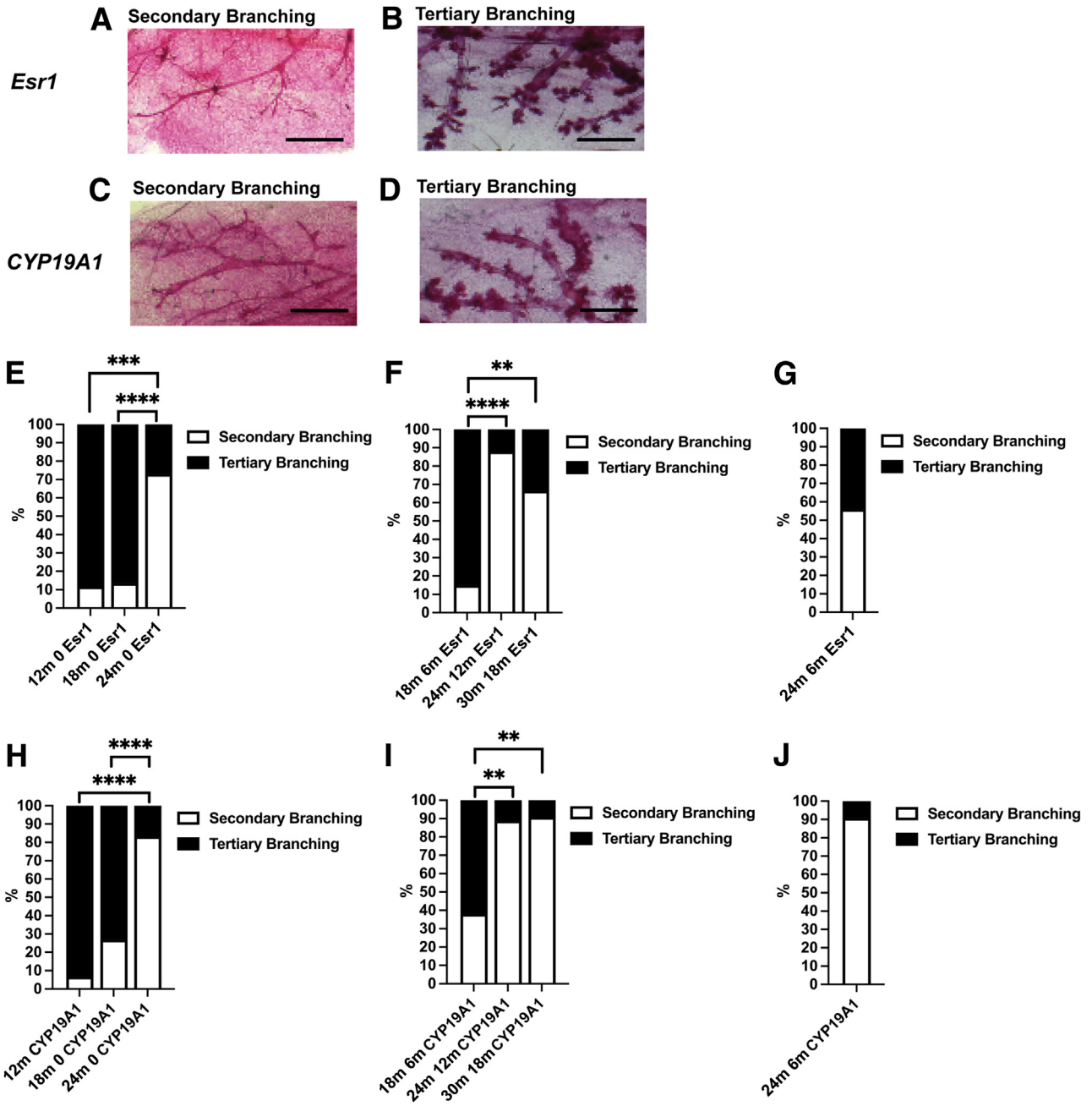

Figure 1 Age and reproductive senescence in mice induce a shift toward simpler secondary mammary gland branching structures. **A:** Representative mammary gland whole mount image of secondary gland in a mouse estrogen receptor 1 (estrogen receptor α; *Esr1*) mouse at age 30 months (m). **B:** Representative mammary gland whole mount image of tertiary branching in an *Esr1* mice at age 30m. **C:** Representative mammary gland whole mount image of secondary branching in a human cytochrome P450 family 19 subfamily A member 1 (aromatase; *CYP19A1*) mice at age 30m. **D:** Representative mammary gland whole mount image of tertiary branching in a *CYP19A1* mice at age 30m. **E:** Bar graphs showing relative percentages of *Esr1* mice with secondary versus tertiary branching on whole mount analyses from cohorts without transgene induction (end points: age 12m $n = 17$, age 18m $n = 22$, age 24m $n = 26$). **F:** Bar graphs showing relative percentages of *Esr1* mice with secondary versus tertiary branching on whole mount analyses from cohorts with transgene induction at age 12 months (end points: age 18m $n = 20$, age 24m $n = 25$, age 30m $n = 18$). **G:** Bar graph showing relative percentages of *Esr1* mice with secondary versus tertiary branching on whole mount analyses from cohort with transgene induction at age 18 months (end point 24m $n = 25$). **H:** Bar graphs showing relative percentages of *CYP19A1* mice with secondary versus tertiary branching on whole mount analyses from cohorts without transgene induction (end points: age 12m $n = 15$, age 18m $n = 26$, age 24m $n = 24$). **I:** Bar graphs showing relative percentages of *CYP19A1* mice with secondary versus tertiary branching on whole mount analyses from cohorts with transgene induction at age 12 months (end points: age 18m $n = 21$, age 24m $n = 18$, age 30m $n = 11$). **J:** Bar graph showing relative percentages of *CYP19A1* mice with secondary versus tertiary branching on whole mount analyses from cohort with transgene induction at age 18 months (end point 24m $n = 22$). $^{**}P < 0.01$, $^{***}P < 0.001$, and $^{****}P < 0.0001$ (Fisher exact test, two sided, GraphPad Prism version 9.4.1). Scale bars = 1000 μm (**A**–**D**). Original magnification, ×0.5 (**A**–**D**).

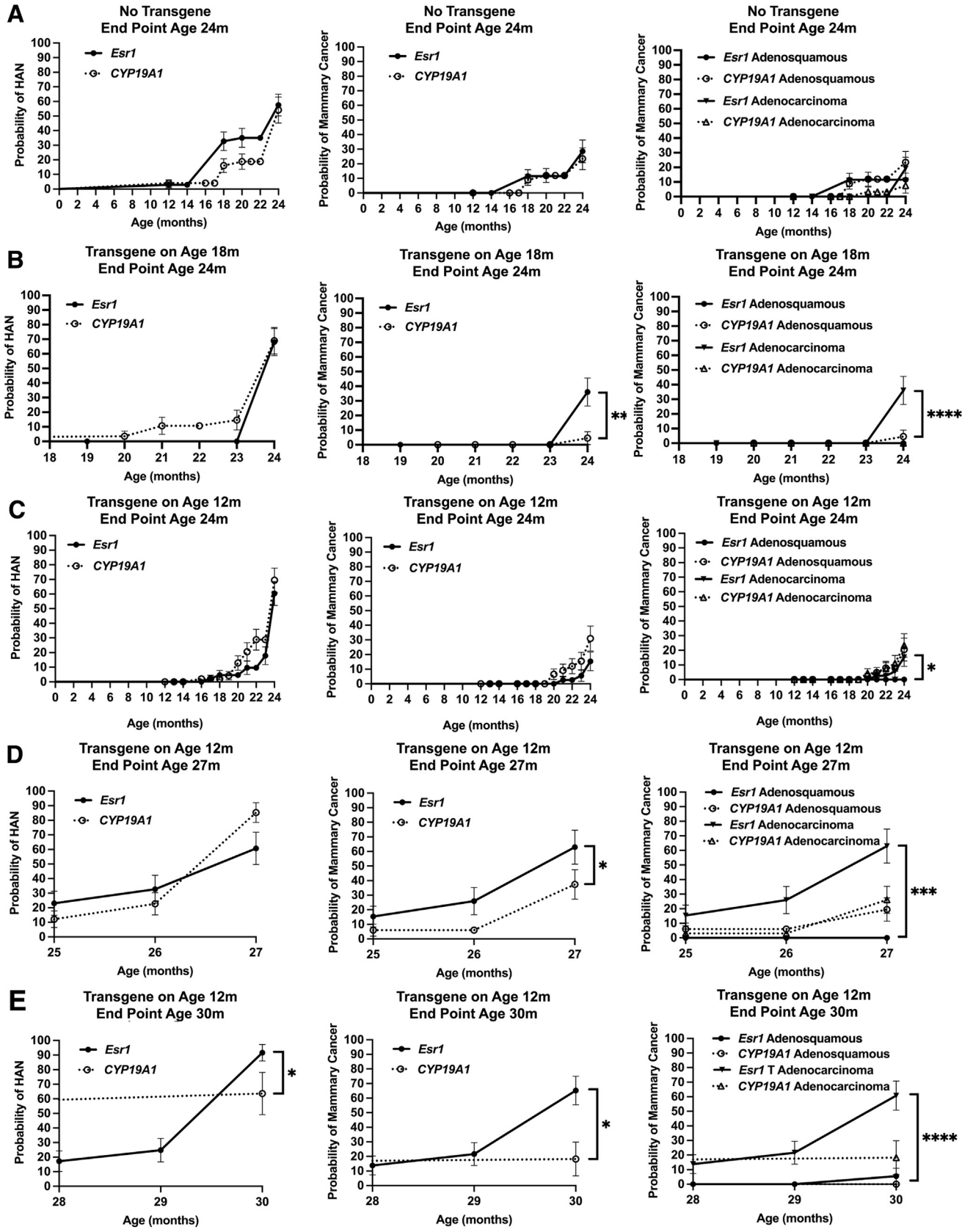
A
No Transgene
End Point Age 24m
Probability of HAN
Esr1
CYP19A1
Age (months)
No Transgene
End Point Age 24m
Probability of Mammary Cancer
Esr1
CYP19A1
Age (months)
No Transgene
End Point Age 24m
Probability of Mammary Cancer
Esr1 Adenosquamous
CYP19A1 Adenosquamous
Esr1 Adenocarcinoma
CYP19A1 Adenocarcinoma
Age (months)
B
Transgene on Age 18m
End Point Age 24m
Probability of HAN
Esr1
CYP19A1
Age (months)
Transgene on Age 18m
End Point Age 24m
Probability of Mammary Cancer
Esr1
CYP19A1
**
Age (months)
Transgene on Age 18m
End Point Age 24m
Probability of Mammary Cancer
Esr1 Adenosquamous
CYP19A1 Adenosquamous
Esr1 Adenocarcinoma
CYP19A1 Adenocarcinoma
****
Age (months)
C
Transgene on Age 12m
End Point Age 24m
Probability of HAN
Esr1
CYP19A1
Age (months)
Transgene on Age 12m
End Point Age 24m
Probability of Mammary Cancer
Esr1
CYP19A1
Age (months)
Transgene on Age 12m
End Point Age 24m
Probability of Mammary Cancer
Esr1 Adenosquamous
CYP19A1 Adenosquamous
Esr1 Adenocarcinoma
CYP19A1 Adenocarcinoma
*
Age (months)
D
Transgene on Age 12m
End Point Age 27m
Probability of HAN
Esr1
CYP19A1
Age (months)
Transgene on Age 12m
End Point Age 27m
Probability of Mammary Cancer
Esr1
CYP19A1
*
Age (months)
Transgene on Age 12m
End Point Age 27m
Probability of Mammary Cancer
Esr1 Adenosquamous
CYP19A1 Adenosquamous
Esr1 Adenocarcinoma
CYP19A1 Adenocarcinoma
***
Age (months)
E
Transgene on Age 12m
End Point Age 30m
Probability of HAN
Esr1
CYP19A1
*
Age (months)
Transgene on Age 12m
End Point Age 30m
Probability of Mammary Cancer
Esr1
CYP19A1
*
Age (months)
Transgene on Age 12m
End Point Age 30m
Probability of Mammary Cancer
Esr1 Adenosquamous
CYP19A1 Adenosquamous
Esr1 T Adenocarcinoma
CYP19A1 Adenocarcinoma
****
Age (months)

necropsy $n = 44$; *CYP19A1* age 12 months entered $n = 17$, end point $n = 15$ (88%), cage death $n = 2$; age 12.25 months entered $n = 6$, end point $n = 6$ (100%); age 18 months entered $n = 29$, end point $n = 26$ (90%), cage death $n = 3$; age 18.25 months entered $n = 6$, end point $n = 5$ (83%), cage death $n = 1$; age 24 months no transgene induction $n = 40$, end point $n = 24$ (60%), cage death $n = 5$, early necropsy $n = 11$; age 24m with 6m transgene induction $n = 41$, end point $n = 22$ (54%), cage death $n = 8$, early necropsy $n = 11$; age 24m with 12m transgene induction $n = 37$, end point $n = 19$ (51%), cage death $n = 7$, early necropsy $n = 11$; and age 30m with 18m transgene induction entered $n = 82$, end point $n = 11$ (13%), cage death $n = 25$, early necropsy $n = 35$. Weights for mice that reached specific cohort age end point: *Esr1*: 12 months 27 ± 1 g, 12.25 months 31 ± 2 g, 18 months 34 ± 2 g, 18.25 months 35 ± 2 g, 24 months no transgene induction 40 ± 2 g, age 24m with 6m transgene induction 54 ± 3 g, age 24m with 12m transgene induction 57 ± 3 g, age 30m with 18m transgene induction 38 ± 3 g. *CYP19A1*: 12 months 30 ± 1 g, 12.25 months 28 ± 1 g, 18 months 30 ± 1 g, 18.25 months 23 ± 1 g, 24 months no transgene induction 33 ± 1 g, age 24m with 6m transgene induction 32 ± 1 g, age 24m with 12m transgene induction 37 ± 2 g, age 30m with 18m transgene induction 32 ± 1 g. Five groups were analyzed for mammary cancer development over time. Each group consisted of all mice necropsied at a specified end point as well as mice in that group subjected to early necropsy (n, mean weight ± SEM): No transgene end point age 24 consisted of mice from age 0 to age 24 months without transgene induction (*Esr1* $n = 70$, 34 ± 2 g; *CYP19A1* $n = 75$, 31 ± 1 g); transgene at age 18 end point age 24 months consisted of mice from age 18 to age 24 months (*Esr1* $n = 27$, 52 ± 3 g; *CYP19A1* $n = 28$, 32 ± 1 g); transgene at age 12 end point age 24 months consisted of mice from age 12 to age 24 months (*Esr1* $n = 48$, 47 ± 3 g; *CYP19A1* $n = 58$, 32 ± 1 g); transgene at age 12 end point age 27 months consisted of mice from age 25 to age 27 months (*Esr1* $n = 26$, 36 ± 3 g; *CYP19A1* $n = 33$, 32 ± 1 g); transgene at age 12 end point age 30 months consisted of mice from age 28 to age 30 months (*Esr1* $n = 29$, 37 ± 2 g; *CYP19A1* $n = 11$, 32 ± 1 g). In preparation for assessing relative transgene expression levels and performance of RNA-sequencing (RNAseq) analyses, thoracic (number 2) mammary glands were flash frozen in liquid nitrogen and stored at −80°C. For each assay, randomly selected glands from each cohort were thawed in Invitrogen Trizol reagent (ThermoFisher Scientific, Waltham, MA) before homogenization using a Qiagen Tissuruptor and Qiashredder (Qiagen, Hilden, Germany). RNA was isolated utilizing the Direct Zol RNA miniprep kit (Zymo Research, Irvine, CA) with quantification on a Qubit 2.0 Fluorometer (Qiagen) and RNA integrity assessed by an Agilent 2100 Bioanalyzer (Agilent, Santa Clara, CA). cDNA was generated using 1 μg of RNA using the High Capacity RNA to cDNA kit (Applied Biosystems, Waltham, MA) and Platinum Taq DNA Polymerase (Invitrogen, Waltham, MA) used for RT-PCR. For *tet-op−Esr1*, two unique primer pairs were used and expression was normalized to β-actin expression levels[28]: Sp3 pair: 5′CCACACCAGCCACCACCTTC3' (forward) and 5′CCACTTCAGCACATTCCTTA3′ (reverse); and Sp4 pair: 5′GATGAGACAGCACAA CAACC3' (forward) and 5′CAAAGGCATGGAGCAT CTCT3' (reverse); predicted sizes were 287 and 385 bp, respectively. For *tet-op−CYP19A1*, one unique primer set was used and expression was normalized to β-actin expression levels[15]: tet-op−CYP19A1: 5′CCTTGCACCCA GATGAGACT3' (forward) and 5′GACAGCACAACAA CCAGCAC3' (reverse); predicted size was 134 bp. Endogenous mouse β-actin: 5ATCGTGGGCCGC CCTAGGCA3' (forward) and 5′TGGCCTTAGGGTT CAGAGGG3' (reverse); predicted size was 244 bp. PCR amplicons were run on 2% agarose E-gels (Invitrogen) with imaging by blue fluorescence on an Amersham Imager 600 (GE HealthCare, Chicago, IL). Relative pixel intensities for amplicon bands for transgene expression were measured,

Figure 2 Mouse estrogen receptor 1 (estrogen receptor α; *Esr1*) overexpression induces mammary adenocarcinomas in aging female mice. **A:** Kaplan-Meier curves of probability of hyperplastic alveolar nodules (HANs), mammary cancers, mammary adenocarcinoma, and mammary adenosquamous cancers in *Esr1* and human cytochrome P450 family 19 subfamily A member 1 (aromatase; *CYP19A1*) mice without transgene induction from birth through age 24 months (m; *Esr1* $n = 70$, *CYP19A1* $n = 75$). **B:** Kaplan-Meier curves of probability of HANs, mammary cancers, mammary adenocarcinoma, and mammary adenosquamous cancers in *Esr1* and *CYP19A1* mice with transgene induction at age 18m, end point age 24m (*Esr1* $n = 27$, *CYP19A1* $n = 28$). **C:** Kaplan-Meier curves of probability of HANs, mammary cancers, mammary adenocarcinoma, and mammary adenosquamous cancers in *Esr1* and *CYP19A1* mice with transgene induction at age 12m, end point age 24m (*Esr1* $n = 48$, *CYP19A1* $n = 56$). **D:** Kaplan-Meier curves of probability of HANs, mammary cancers, mammary adenocarcinoma, and mammary adenosquamous cancers in *Esr1* and *CYP19A1* mice with transgene induction at age 12m, end point age 27m (*Esr1* $n = 26$, *CYP19A1* $n = 33$). **E:** Kaplan-Meier curves of probability of HANs, mammary cancers, mammary adenocarcinoma, and mammary adenosquamous cancers in *Esr1* and *CYP19A1* mice with transgene induction at age 12m, end point age 30m (*Esr1* $n = 29$, *CYP19A1* $n = 11$). Cumulative number (percentage) for each cohort: *Esr1* no transgene 24m: adenocarcinoma $n = 5$ (19%), adenosquamous $n = 6$ (12%). *CYP19A1* no transgene: 24m $n = 2$ (8%), adenosquamous $n = 9$ (23%). *Esr1* transgene induction at age 18m, end point 24m: adenocarcinoma $n = 9$ (36%), adenosquamous $n = 0$. *CYP19A1* transgene induction at age 18m, end point 24m: adenocarcinoma $n = 0$, adenosquamous $n = 1$ (5%). *Esr1* transgene induction at age 12m, end point 24m: adenocarcinoma $n = 5$ (15%), adenosquamous $n = 0$. *CYP19A1* transgene induction at age 12m, end point 24m: adenocarcinoma $n = 7$ (23%), adenosquamous $n = 6$ (21%). *Esr1* transgene induction at age 12m, end point 27m: adenocarcinoma $n = 12$ (63%), adenosquamous $n = 0$. *CYP19A1* transgene induction at age 12m, end point 27m: adenocarcinoma $n = 6$ (26%), adenosquamous $n = 5$ (19%). *Esr1* transgene induction at age 12m, end point 30m: adenocarcinoma $n = 15$ (61%), adenosquamous $n = 1$ (6%). *CYP19A1* transgene induction at age 12m, end point 30m: adenocarcinoma $n = 2$ (18%), adenosquamous $n = 0$. $^*P < 0.05$, $^{**}P < 0.01$, $^{***}P < 0.001$, and $^{****}P < 0.0001$ [log-rank (Mantel-Cox) test, GraphPad Prism version 9.4.0].

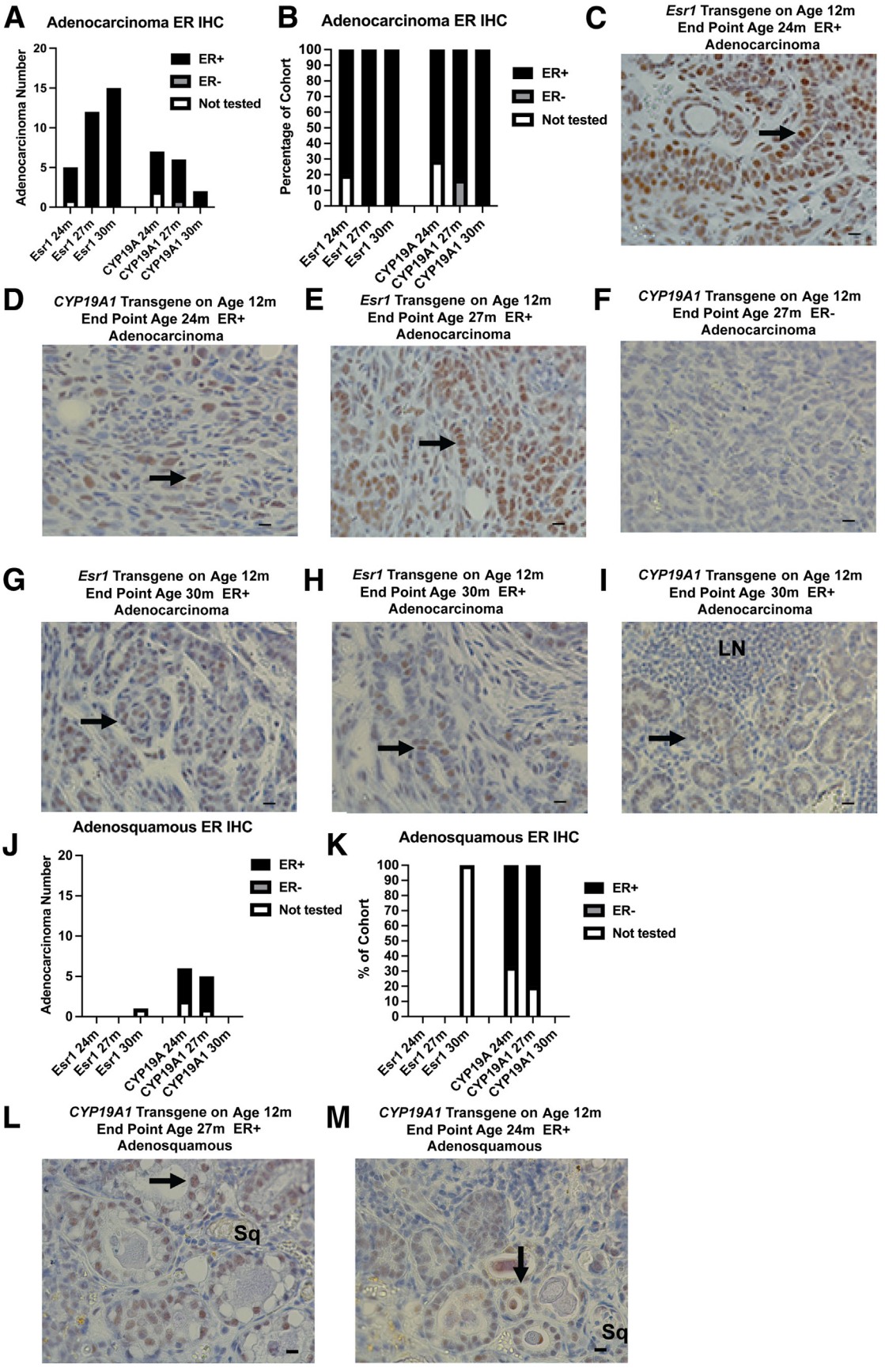
A
Adenocarcinoma ER IHC
Adenocarcinoma Number
ER+
ER-
Not tested
Esr1 24m
Esr1 27m
Esr1 30m
CYP19A 24m
CYP19A1 27m
CYP19A1 30m
B
Adenocarcinoma ER IHC
Percentage of Cohort
C
Esr1 Transgene on Age 12m
End Point Age 24m ER+
Adenocarcinoma
D
CYP19A1 Transgene on Age 12m
End Point Age 24m ER+
Adenocarcinoma
E
Esr1 Transgene on Age 12m
End Point Age 27m ER+
Adenocarcinoma
F
CYP19A1 Transgene on Age 12m
End Point Age 27m ER-
Adenocarcinoma
G
Esr1 Transgene on Age 12m
End Point Age 30m ER+
Adenocarcinoma
H
Esr1 Transgene on Age 12m
End Point Age 30m ER+
Adenocarcinoma
I
CYP19A1 Transgene on Age 12m
End Point Age 30m ER+
Adenocarcinoma
LN
J
Adenosquamous ER IHC
Adenocarcinoma Number
K
Adenosquamous ER IHC
% of Cohort
L
CYP19A1 Transgene on Age 12m
End Point Age 27m ER+
Adenosquamous
Sq
M
CYP19A1 Transgene on Age 12m
End Point Age 24m ER+
Adenosquamous
Sq

followed by normalization to the concurrent β-actin amplicon band for each sample to determine relative transgene expression levels (Adobe Photoshop version 23.5.0, San Jose, CA). Fold induction at 1 week compared with baseline was calculated for each genotype independently at ages 12 and 18 months.

Mammary Gland Whole Mount Analysis

Carmine-alum–stained inguinal (number 4) mammary gland whole mounts were prepared,[29] and visually examined with images taken at ×0.5 utilizing a Nikon Eclipse E800M microscope with a Nikon DXM1200 camera (Nikon Instruments, Inc., Melville, NY). Each whole mount was blindly scored by 2 to 4 independent observers (P.A.F, W.W., B.L.R., V.M., or J.W.) for secondary versus tertiary branching structure.[30] Hyperplastic alveolar nodule (HAN) numbers were counted.[31] The final score was the majority score, with images re-examined and final score set by P.A.F in the event of tied scores.

Histology and ER α Immunohistochemistry

Inguinal (number 4) mammary glands were fixed in 10% neutral formalin solution and embedded in paraffin, and tissue longitudinal midgland sections (5 μm thick) were used for hematoxylin and eosin staining and ER α immunohistochemistry. Hematoxylin and eosin slides from all cohorts were read blindly and scored for presence of adenocarcinoma or adenosquamous carcinomas (P.A.F. or W.W.). ER α protein expression in adenocarcinomas and adenosquamous carcinomas was evaluated by ER immunohistochemistry. ER α protein was detected utilizing rabbit polyclonal anti–estrogen receptor α (catalog number 06-935; Millipore Sigma, Burlington, MA), 1:4800, 1 hour, room temperature. Heat-induced epitope retrieval was performed by immersing tissue sections at 98°C for 20 minutes in 10 mmol/L citrate buffer (pH 6.0) with 0.05% Tween followed by treatment with 3% hydrogen peroxide and 10% normal goat serum (10 minutes each) before application of primary antibody. After primary antibody exposure, slides were exposed to a horseradish peroxidase–labeled polymer [30 minutes; EnVision+ System-HRP Labeled Polymer Anti-Rabbit, K4003 (Agilent, Dako, Carpinteria, CA)] and 3′-diaminobenzidine (5 minutes, Agilent, Dako) and counterstained with hematoxylin (Harris Modified Hematoxylin; Fisher Scientific, Hampton, NH). ER α immunohistochemistry was read by P.A.F. Digital images were taken at ×40 utilizing a Nikon Eclipse E800M microscope with a Nikon DXM1200 camera.

RNAseq Analysis

Flash frozen thoracic (number 2) mammary glands were stored at −80°C, thawed in Invitrogen Trizol reagent (ThermoFisher Scientific), and homogenized using a Qiagen Tissuruptor and Qiashredder (Qiagen). RNA was isolated using Direct Zol RNA miniprep kit (Zymo Research), quantified on a Qubit 2.0 or 4.0 Fluorometer (Qiagen), and analyzed for RNA integrity using the Agilent 2100 Bioanalyzer. Indexed, single-index sequencing libraries were prepared from 1 μg ribosome depleted total RNA using TruSeq Stranded Total RNA Library Preparation Human/Mouse/Rat (Illumina, San Diego, CA). Sequencing was performed using the Illumina NextSeq 550, SE 75-bp read length; minimum reads ≥50 mol/L per sample. Sequencing quality was checked using FastQC processing version 0.11.9 (*https://www.bioinformatics.babraham.ac.uk/projects/fastqc*, last accessed October 30, 2022). Contaminated adaptor and/or low-quality portions of

Figure 3 Mammary adenocarcinomas developing in aged mice are predominantly estrogen receptor α (ER)–positive. **A:** Bar graphs illustrating numbers of adenocarcinomas identified in mouse estrogen receptor 1 (estrogen receptor α; *Esr1*) and human cytochrome P450 family 19 subfamily A member 1 (aromatase; *CYP19A1*) mice with transgene expression induced at age 12 months (m) analyzed by end points 24, 27, and 30m. ER immunohistochemistry (IHC) used to characterize adenocarcinomas as ER positive (+) or negative (−). Numbers of samples not tested indicated. (Total number of adenocarcinomas: *Esr1* 24m $n = 5$, *Esr1* 27m $n = 12$, *Esr1* 30m $n = 15$, *CYP19A1* 24m $n = 7$, *CYP19A1* 27m $n = 6$, *CYP19A1* $n = 2$). **B:** Bar graphs illustrating percentages of ER$^+$, ER$^-$, and not tested adenocarcinomas from *Esr1* and *CYP19A1* mice with transgene expression induced at age 12m analyzed by end points 24, 27, and 30m. Percentage established as ER$^+$: *Esr1* 24m 80%, *Esr1* 27m 100%, *Esr1* 30m 100%, *CYP19A1* 24m 71%, *CYP19A1* 27m 83%, *CYP19A1* 30m 100%. Percentage established as ER$^-$: *CYP19A1* 27m 17%. Overall: *Esr1*: $n = 31$ tested, 100% ER$^+$. *CYP19A1*: $n = 13$ tested, 92% ER$^+$, 8% ER$^-$. **C:** Representative image of ER$^+$ mammary adenocarcinoma from *Esr1* mouse with transgene induction age 12m, end point age 24m. **D:** Representative image of ER$^+$ mammary adenocarcinoma from *CYP19A1* mouse with transgene induction age 12m, end point age 24m. **E:** Representative image of ER$^+$ mammary adenocarcinoma from *Esr1* mouse with transgene induction age 12m, end point age 27m. **F:** Representative image of ER$^-$ mammary adenocarcinoma from *CYP19A1* mouse with transgene induction age 12m, end point age 27m. **G:** Representative image of ER$^+$ mammary adenocarcinoma from *Esr1* mouse with transgene induction age 12m, end point age 30m. **H:** Representative image of ER$^+$ mammary adenocarcinoma from *Esr1* mouse with transgene induction age 12m, end point age 30m. **I:** Representative image of ER$^+$ mammary adenocarcinoma from *CYP19A1* mouse with transgene induction age 12m, end point age 30m. **J:** Bar graphs illustrating numbers of adenosquamous carcinomas identified in *Esr1* and *CYP19A1* mice with transgene expression induced at age 12m analyzed by end points 24, 27, and 30m. ER immunohistochemistry used to characterize adenocarcinomas as ER$^+$ and ER$^-$. Number of samples not tested indicated. (Total number of adenosquamous carcinomas: *Esr1* 24, 27m $n = 0$, *Esr1* 30m $n = 1$, *CYP19A1* 24m $n = 6$, *CYP19A1* 27m $n = 5$, *CYP19A1* 30m $n = 0$). **K:** Bar graphs illustrating percentages of ER$^+$, ER$^-$, and not tested adenosquamous carcinomas from *Esr1* and *CYP19A1* mice with transgene expression induced at age 12m analyzed by end points 24, 27, and 30m. Percentage established as ER$^+$: *CYP19A1* 24m 67%, *CYP19A1* 27m 80%. Overall: *CYP19A1*: $n = 8$ tested, 100% ER$^+$. **L:** Representative image of ER$^+$ mammary adenosquamous carcinoma from *CYP19A1* mouse with transgene induction age 12m, end point age 24m. **M:** Representative image of ER$^+$ mammary adenosquamous carcinoma from *CYP19A1* mouse with transgene induction age 12m, end point age 27m. **Black arrows** indicate representative cells with nuclear localized ER staining. Scale bars = 10 μm (**C**–**I**, **L**, and **M**). Original magnification, ×40 (**C**–**I**, **L**, and **M**). LN, lymph node; Sq, squamous component of an adenosquamous cancer.

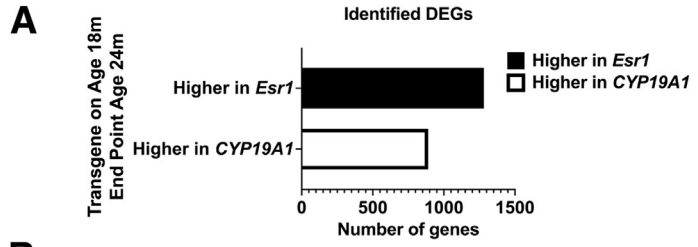
A
Identified DEGs
Transgene on Age 18m
End Point Age 24m
Higher in Esr1
Higher in CYP19A1
Higher in Esr1
Higher in CYP19A1
0
500
1000
1500
Number of genes

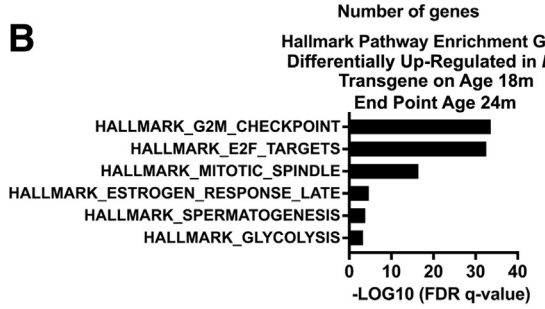
B
Hallmark Pathway Enrichment Genes
Differentially Up-Regulated in Esr1
Transgene on Age 18m
End Point Age 24m
HALLMARK_G2M_CHECKPOINT
HALLMARK_E2F_TARGETS
HALLMARK_MITOTIC_SPINDLE
HALLMARK_ESTROGEN_RESPONSE_LATE
HALLMARK_SPERMATOGENESIS
HALLMARK_GLYCOLYSIS
0
10
20
30
40
-LOG10 (FDR q-value)

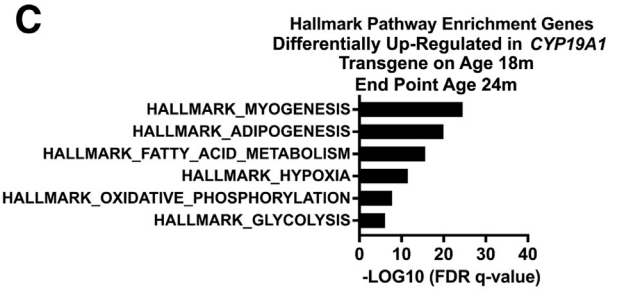
C
Hallmark Pathway Enrichment Genes
Differentially Up-Regulated in CYP19A1
Transgene on Age 18m
End Point Age 24m
HALLMARK_MYOGENESIS
HALLMARK_ADIPOGENESIS
HALLMARK_FATTY_ACID_METABOLISM
HALLMARK_HYPOXIA
HALLMARK_OXIDATIVE_PHOSPHORYLATION
HALLMARK_GLYCOLYSIS
0
10
20
30
40
-LOG10 (FDR q-value)

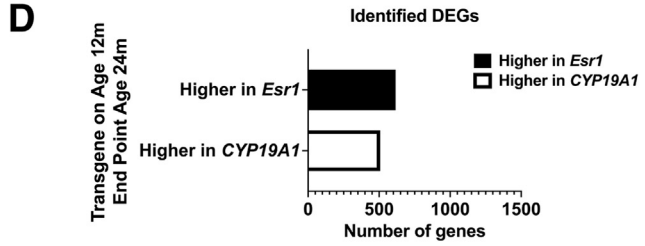
D
Identified DEGs
Transgene on Age 12m
End Point Age 24m
Higher in Esr1
Higher in CYP19A1
Higher in Esr1
Higher in CYP19A1
0
500
1000
1500
Number of genes

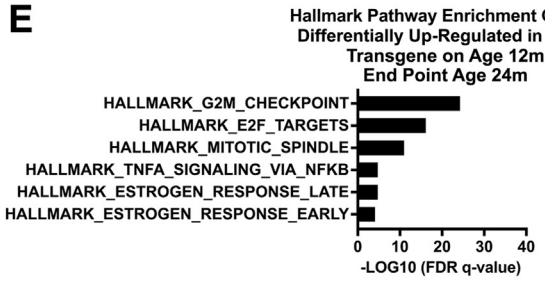
E
Hallmark Pathway Enrichment Genes
Differentially Up-Regulated in Esr1
Transgene on Age 12m
End Point Age 24m
HALLMARK_G2M_CHECKPOINT
HALLMARK_E2F_TARGETS
HALLMARK_MITOTIC_SPINDLE
HALLMARK_TNFA_SIGNALING_VIA_NFKB
HALLMARK_ESTROGEN_RESPONSE_LATE
HALLMARK_ESTROGEN_RESPONSE_EARLY
0
10
20
30
40
-LOG10 (FDR q-value)

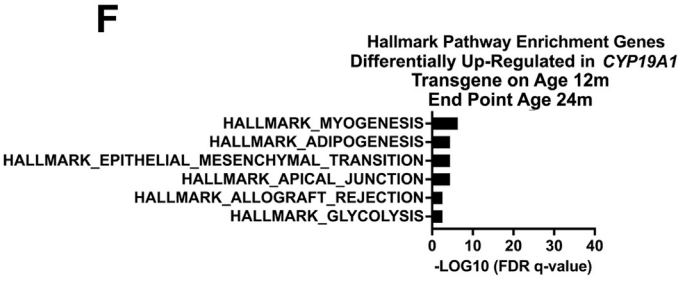
F
Hallmark Pathway Enrichment Genes
Differentially Up-Regulated in CYP19A1
Transgene on Age 12m
End Point Age 24m
HALLMARK_MYOGENESIS
HALLMARK_ADIPOGENESIS
HALLMARK_EPITHELIAL_MESENCHYMAL_TRANSITION
HALLMARK_APICAL_JUNCTION
HALLMARK_ALLOGRAFT_REJECTION
HALLMARK_GLYCOLYSIS
0
10
20
30
40
-LOG10 (FDR q-value)

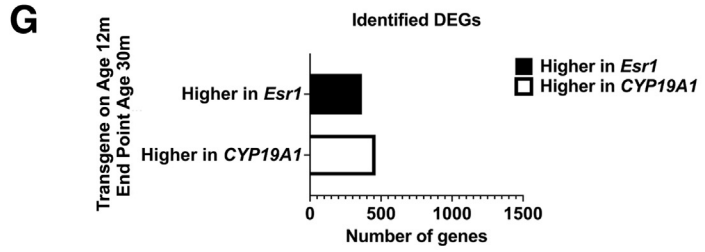
G
Identified DEGs
Transgene on Age 12m
End Point Age 30m
Higher in Esr1
Higher in CYP19A1
Higher in Esr1
Higher in CYP19A1
0
500
1000
1500
Number of genes

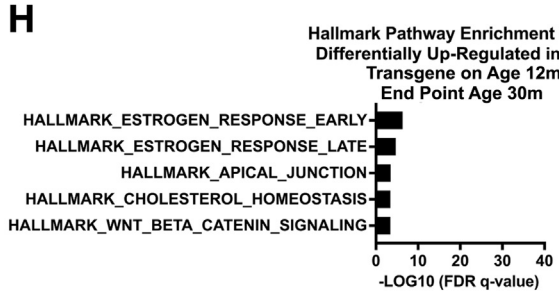
H
Hallmark Pathway Enrichment Genes
Differentially Up-Regulated in Esr1
Transgene on Age 12m
End Point Age 30m
HALLMARK_ESTROGEN_RESPONSE_EARLY
HALLMARK_ESTROGEN_RESPONSE_LATE
HALLMARK_APICAL_JUNCTION
HALLMARK_CHOLESTEROL_HOMEOSTASIS
HALLMARK_WNT_BETA_CATENIN_SIGNALING
0
10
20
30
40
-LOG10 (FDR q-value)

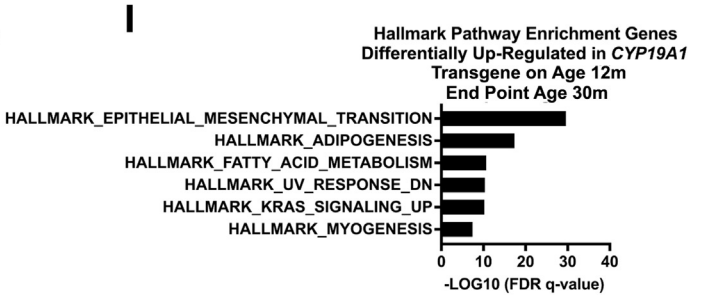
I
Hallmark Pathway Enrichment Genes
Differentially Up-Regulated in CYP19A1
Transgene on Age 12m
End Point Age 30m
HALLMARK_EPITHELIAL_MESENCHYMAL_TRANSITION
HALLMARK_ADIPOGENESIS
HALLMARK_FATTY_ACID_METABOLISM
HALLMARK_UV_RESPONSE_DN
HALLMARK_KRAS_SIGNALING_UP
HALLMARK_MYOGENESIS
0
10
20
30
40
-LOG10 (FDR q-value)

sequenced reads were trimmed using Trim Galore version 0.6.5 (*https://github.com/FelixKrueger/TrimGalore*, last accessed August 28, 2022). Trimmed reads were aligned to the reference mouse genome (mm10), using STAR version 2.7.9a.[32] The batch effect was normalized using RUVSeq version 1.26.0 with the RUVg method.[33] Normalized expression levels were estimated by means of transcripts per million (TPM) using RSEM version 1.3.1.[34] Differentially expressed genes (DEGs) between genotypes at each end point were identified using DESeq2.[35] Genes were considered statistically significantly differentially expressed when adjusted $P < 0.05$. Protein coding DEGs between models at each end point were identified, and numbers visualized as expressed higher in *Esr1* versus *CYP19A1* mice using bar graphs with each group analyzed independently for enrichment in HALLMARK gene sets (Gene Set Enrichment Analysis, Molecular Signatures Database version 7.5.1, *http://www.gsea-msigdb.org*, last accessed June 21, 2022).[36,37] Bar graphs for presentation of false discovery rate q-values and gene expression levels by TPM for HALLMARK_ESTROGEN_RESPONSE_LATE genes and heat maps for visualization of relative gene expression levels of DEGs between models that overlapped with the Prosigna PAM50 gene set[6] were prepared using GraphPad Prism version 9.4 (GraphPad Software, San Diego, CA). RNAseq data generated as part of this study were deposited in National Center for Biotechnology Information's Gene Expression Omnibus[38] and are accessible through series accession number GSE201767 (*https://www.ncbi.nlm.nih.gov/geo/query/acc.cgi?acc=GSE201767*, last accessed August 24, 2022).

Ovarian Follicle Counts

Ovarian follicle counts were determined by histologic evaluation after paraformaldehyde fixation, paraffin embedding, and hematoxylin and eosin staining of microtome sections of ovaries taken every 8 μm.[39,40] Total numbers of primordial follicles, primary follicles, preantral follicles, and antral follicles were counted on every 10th section blindly without knowledge of identity. Definition of follicles is as follows: primordial follicles: follicles with an oocyte, surrounded by a single layer of squamous granulosa cells; primary follicles: follicles that consist of an oocyte, surrounded by a single layer of cuboidal granulosa cells; preantral follicles: follicles containing an oocyte, surrounded by multiple layers of cuboidal granulosa cells and theca cells; and antral follicles: follicles that consist of an oocyte, surrounded by numerous layers of cuboidal granulosa cells, theca cells, and a fluid-filled antrum. Preantral and antral follicles were required to have nuclear material present to avoid double counting. Total number of follicles and number and percentage of each type of follicle were recorded.

Statistical Analysis

Calculation of means and SEMs, generation of scatterplots, bar graphs, and heat maps, evaluation of nonrandom associations between tertiary and secondary branching using Fisher exact test, generation of Kaplan-Meier curves, and statistical analysis for significant differences by the log-rank (Mantel-Cox) test and two-way analyses of variance were performed utilizing GraphPad Prism version 9.4.1. The number of asterisks applied indicates significance levels of $*P < 0.05$, $**P < 0.01$, $***P < 0.001$, and $****P < 0.0001$. $P < 0.05$ was considered statistically significant for all comparisons.

Results

Reproductive Senescence Significantly Alters Mammary Gland Branching Patterns

Ovarian follicle counts were assessed over time to determine the age when mice of each genotype entered into reproductive senescence. Both *Esr1* and *CYP19A1* mice entered into reproductive senescence by age 18 months with significantly diminished follicle counts appearing with advancing age (Supplemental Figure S1). The appearance of secondary and tertiary branching patterns was similar in *Esr1* and *CYP19A1* mice (Figure 1, A–D). The proportion of mice exhibiting tertiary branching decreased significantly with age and advancement through reproductive senescence

Figure 4 At age 24 months (m), mouse estrogen receptor 1 (estrogen receptor α; *Esr1*) transgene induction is associated with significantly elevated expression of cell proliferation genes. **A:** Bar graph presenting numbers of significantly differentially expressed genes (DEGs) in *Esr1* and human cytochrome P450 family 19 subfamily A member 1 (aromatase; *CYP19A1*) mice with transgene induction at age 18m, end point age 24m (adjusted $P < 0.05$, DESeq2). **B:** Bar graph presenting the six HALLMARK gene sets with the lowest false discovery rate (FDR) q-values identified from significant DEGs expressed at higher levels in *Esr1* mice with transgene induction at age 18m, end point age 24m. **C:** Bar graph presenting the six HALLMARK gene sets with the lowest significant FDR q-values identified from significant DEGs expressed at higher levels in *CYP19A1* mice with transgene induction at age 18m, end point age 24m. **D:** Bar graph presenting numbers of significantly differentially expressed genes in *Esr1* and *CYP19A1* mice with transgene induction at age 12m, end point age 24m (adjusted $P < 0.05$, DESeq2). **E:** Bar graph presenting the six HALLMARK gene sets with the lowest significant FDR q-values identified from significant DEGs expressed at higher levels in *Esr1* mice with transgene induction at age 12m, end point age 24m. **F:** Bar graph presenting the six HALLMARK gene sets with the lowest significant FDR q-values identified from significant DEGs expressed at higher levels in *CYP19A1* mice with transgene induction at age 12m, end point age 24m. **G:** Bar graph presenting numbers of significantly differentially expressed genes in *Esr1* and *CYP19A1* mice with transgene induction at age 12m, end point age 30m (adjusted $P < 0.05$, DESeq2). **H:** Bar graph presenting the six HALLMARK gene sets with the lowest significant FDR q-values identified from significant DEGs expressed at higher levels in *Esr1* mice with transgene induction at age 12m, end point age 30m. **I:** Bar graph presenting the six HALLMARK gene sets with the lowest significant FDR q-values identified from significant DEGs expressed at higher levels in *CYP19A1* mice with transgene induction at age 12m, end point age 30m. Hallmark gene sets identified from Molecular Signatures Database version 7.51 (*http://www.gsea-msigdb.org/gsea/index.jsp*, last accessed June 21, 2022).

in both models (Figure 1, E–J). Notably, even as secondary branching predominated with age, tertiary branching persisted in a small percentage of 30-month–old mice of both genotypes, even though reproductive senescence was completed (Figure 1, F and I). *Esr1* mice demonstrated a significantly higher prevalence of tertiary branching (44%) than *CYP19A1* mice (9%) at age 24 months following 6 months of transgene induction beginning at 18 months of age ($P = 0.0098$, Fisher exact test, GraphPad Prism version 9.4.1) (Figure 1, G and J). No significant differences in follicle counts between mice with and without transgene induction were found (data not shown).

Esr1 Transgene Induction Is Associated with a More Significant Increase in Mammary Adenocarcinoma Prevalence with Age than *CYP19A1* Transgene Induction

To study the impact of age and transgene expression on development of mammary preneoplasia and neoplasia, prevalence rates of HANs and mammary cancer were determined by examination of mammary gland whole mounts and hematoxylin and eosin sections of mammary tissue. In the absence of transgene induction by 24 months, there was no significant difference in HAN or mammary cancer prevalence or distribution of mammary cancer histology between adenocarcinoma and adenosquamous carcinomas (Figure 2A). An age-related increase in prevalence of both preneoplasia and neoplasia was seen, and both models exhibited a significant proportion of adenosquamous carcinomas in the absence of transgene induction (*Esr1* 55%, *CYP19A1* 82%). Transgene induction at age 18 months resulted in a significant difference between the models in mammary cancer, although not HAN, prevalence at age 24 months (Figure 2B). All mammary cancers that developed in the presence of *Esr1* transgene induction were adenocarcinomas, whereas the one mammary cancer found in *CYP19A1* mice exhibited adenosquamous histology. A more extended period of transgene induction beginning at age 12 months was associated with development of mammary adenocarcinomas in both *Esr1* and *CYP19A1* mice aged 24 months (Figure 2C). *Esr1* mice developed only adenocarcinomas, whereas histology of the mammary cancers that developed in the *CYP19A1* mice was evenly divided between adenocarcinomas and adenosquamous carcinomas. Examination of mice between 25 and 27 months of age following transgene induction at age 12 months similarly revealed a significantly higher prevalence of mammary adenocarcinomas in the *Esr1* mice, with histology again divided between adenocarcinoma and adenosquamous carcinoma in the *CYP19A1* mice (Figure 2D). At age 30 months with transgene initiation at age 12 months, *Esr1* mice showed significantly higher prevalence of HANs and mammary adenocarcinomas than *CYP19A1* mice (Figure 2E). In summary, time course experiments demonstrated that *Esr1* transgene induction at either 12 or 18 months of age was reproducibly associated with a higher prevalence of mammary adenocarcinomas than *CYP19A1* transgene induction.

Mammary Cancers Are Predominantly Estrogen Receptor α–Positive

Immunohistochemistry was performed to determine whether the mammary cancers that developed in the *Esr1* and *CYP19A1* mice were ER^+ or ER^-. Cancers were considered ER^+ if they exhibited nuclear-localized estrogen receptor α staining in ≥1% of the cells. Most adenocarcinomas found in the 24- to 30-month–old *Esr1* and *CYP19A1* mice were ER^+ (Figure 3, A and B). One adenocarcinoma that developed in a *CYP19A1* mouse was ER^-. Notably, in all cancers tested, the percentage of cells exhibiting nuclear-localized ER staining was significantly >1%, with most exhibiting a large percentage of ER^+ cells (Figure 3, C–I). The adenosquamous carcinomas that developed in the *CYP19A1* mice were also ER^+ (Figure 3, J–M). This experiment demonstrated that a high proportion of the mammary cancers that developed in the aged *Esr1* and *CYP19A1* mice showed a high percentage of cells with ER positivity.

Esr1 Transgene Induction Is Associated with Significantly Increased Expression Levels of Cell Proliferation–Related Genes

To test whether the significantly higher prevalence of ER^+ mammary adenocarcinomas in the *Esr1* compared with *CYP19A1* mice was associated with significant transcriptome differences, RNAseq was performed on whole mammary gland tissue without palpable or visual tumor selected randomly before histologic analyses. At age 24 months following 6 months transgene expression, 2172 protein-coding significant DEGs were identified (adjusted $P < 0.05$, DESeq2), 1282 expressed at higher levels in *Esr1* and 890 in *CYP19A1* mice (Figure 4A). DEGs in *Esr1* mice were prominently enriched in HALLMARK gene sets related to cell proliferation (HALLMARK_G2M_CHECKPOINT, HALLMARK_E2F TARGETS, and HALLMARK_MITOTIC SPINDLE), whereas DEGs higher in *CYP19A1* mice were most significantly enriched in HALLMARK_MYOGENESIS, HALLMARK_ADIPOGENESIS, and HALLMARK_FATTY_ACID_METABOLISM (Figure 4, B and C). At age 12 months following 12 months of transgene expression, only 1122 protein-coding DEGs were identified, with 615 higher in *Esr1* and 507 higher in *CYP19A1* mice (adjusted $P < 0.05$, DESeq2) (Figure 4D). The most significant gene enrichment sets in *Esr1* mice were again HALLMARK_G2M_CHECKPOINT, HALLMARK_E2F TARGETS, and HALLMARK_MITOTIC SPINDLE (Figure 4E). HALLMARK_MYOGENESIS and HALLMARK_ADIPOGENESIS were again the most significant gene sets in *CYP19A1* mice, with the third most significant gene set being HALLMARK_EPITHELIAL_MESENCHYMAL_TRANSITION (Figure 4F). At age 30 months

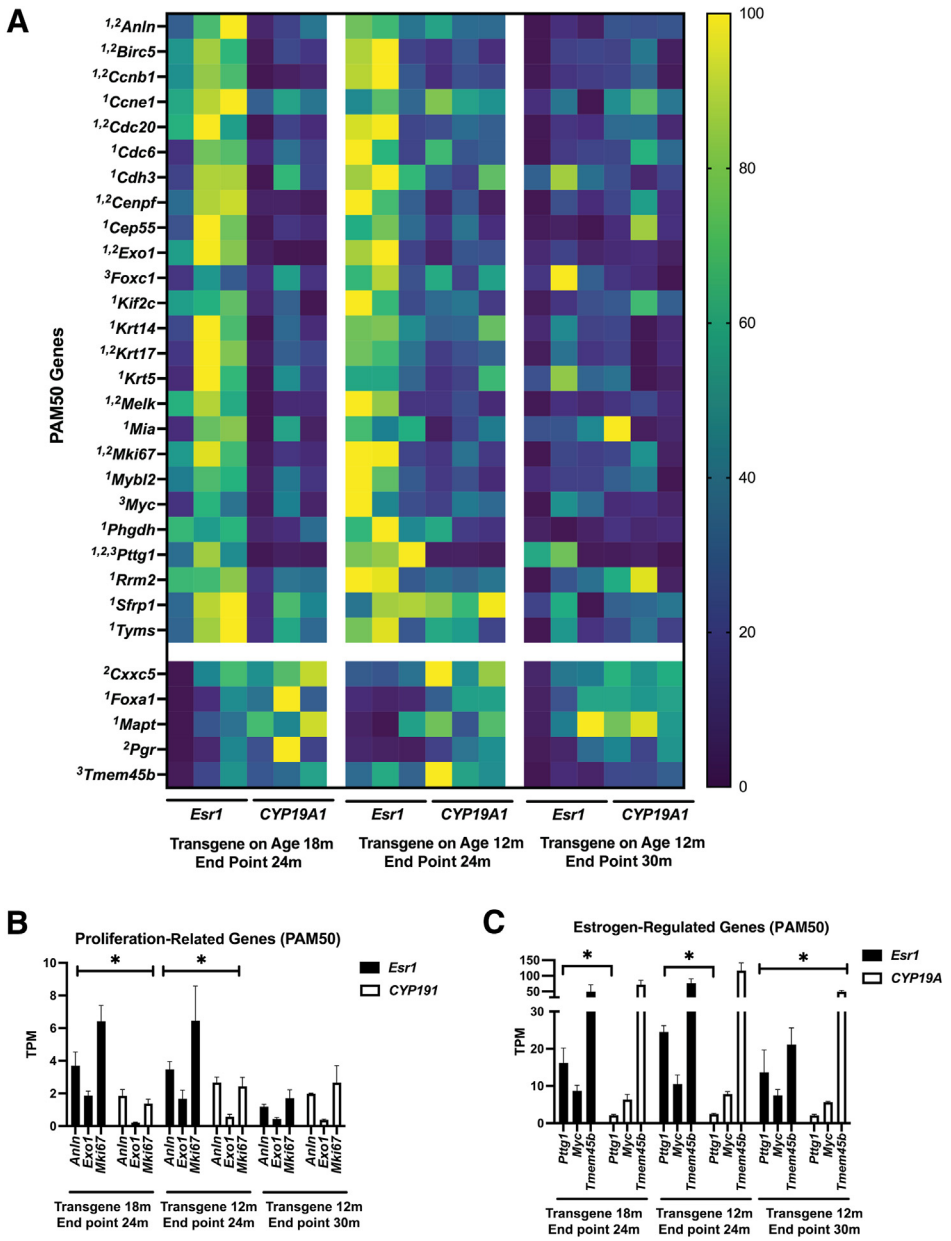

Figure 5 At age 24 months (m), mouse estrogen receptor 1 (estrogen receptor α; *Esr1*) transgene induction is associated with significantly elevated expression of genes linked to a prognostic risk profile for human estrogen receptor α—positive (ER$^+$) breast cancer. **A:** Heat map comparing relative expression levels of significantly differentially expressed genes (DEGs) that are members of the human ER$^+$/HER2$^-$ breast cancer prognostic Prediction Analysis of Microarray (PAM) 50 profile in *Esr1* and human cytochrome P450 family 19 subfamily A member 1 (aromatase; *CYP19A1*) mice with transgene induction age 18m, end point age 24m, and transgene induction at age 12m, end points age 24 and 30 months. 1: Adjusted $P < 0.05$, DESeq2, *Esr1* and *CYP19A1* mice, transgene induction at age 18m, end point age 24m. 2: Adjusted $P < 0.05$, DESeq2, *Esr1* and *CYP19A1* mice, transgene induction at age 12m, end point age 24m. 3: Adjusted $P < 0.05$, DESeq2, *Esr1* and *CYP19A1* mice, transgene induction at age 12m, end point age 30m. Relative expression levels shown for unique individual samples ($n = 3$ for each cohort). Yellow indicates highest expression level, and dark blue indicates lowest expression level, for each gene. **B:** Bar graphs illustrating transcripts per million (TPM) expression levels of three representative proliferation-related genes [anillin, actin-binding protein (*Anln*), exonuclease 1 (*Exo1*), and marker of proliferation Ki-67 (*Mki67*)] from the PAM50 profile in *Esr1* and *CYP19A1* mice at 24 and 30 months of age. Bi-directional bracket ends indicate all three genes expressed at significantly different levels between genotypes. **C:** Bar graphs illustrating TPM expression levels of three representative estrogen-regulated genes [PTTG1 regulator of sister chromatid separation, securin (*Pttg1*), MYC proto-oncogene, BHLH transcription factor (*Myc*), and transmembrane protein 45B (*Tmem45b*)] from the PAM50 profile in *Esr1* and *CYP19A1* mice at 24 and 30 months of age. Down-only bracket ends indicate single gene, and bidirectional bracket ends indicate all three genes expressed at significantly different levels between genotypes. Data are given as means ± SEM (**B** and **C**). *Adjusted $P < 0.05$ (DESeq2). *Birc5*, baculoviral IAP repeat containing 5; *Ccnb1*, cyclin B1; *Ccne1*, cyclin E1; *Cdc20*, cell division cycle 20; *Cdc6*, cell division cycle 6; *Cdh3*, cadherin 3; *Cenpf*, centromere protein F; *Cep55*, centrosomal protein 55; *Cxxc5*, CXXC finger protein 5; E2F, E2 transcription factor; *Foxa1*, forkhead box A1; *Foxc1*, forkhead box C1; G2M, G_2 phase; *Kif2c*, kinesin family member 2; KRAS, Kirsten rat sarcoma viral oncogene homolog; *Krt14*, keratin 14; *Krt17*, keratin 17; *Krt5*, keratin 5; *Mapt*, microtubule-associated protein tau; *Melk*, maternal embryonic leucine zipper kinase; *Mia*, MIA SH3 domain containing; *Mybl2*, MYB proto-oncogene like 2; NFKB, NF-κB; *Pgr*, progesterone receptor; *Phgdh*, phosphoglycerate dehydrogenase; *Rrm2*, ribonucleotide reductase regulatory subunit M2; *Sfrp1*, secreted frizzled-related protein 1; TNFA, tumor necrosis factor-α; *Tyms*, thymidylate synthetase; WNT, wingless/integrated.

following 18 months of transgene expression, 828 significant DEGs were found, with 366 expressed at higher levels in *Esr1* and 462 at higher levels in *CYP19A1* mice (adjusted $P < 0.05$, DESeq2) (Figure 4G). At this age, HALLMARK_ESTROGEN EARLY and HALLMARK_ESTROGEN LATE were the most significant gene enrichment sets in the *Esr1* mice, whereas the most significant enrichment for the *CYP19A1* mice was HALLMARK_EPITHELIAL_MESENCHYMAL_TRANSITION (Figure 4, H and I). Taken together, with age and duration of transgene expression, there was a step-wise decrease in overall numbers of DEGs with cell proliferation–related gene sets relatively enriched in the *Esr1* mice at age 24 months and estrogen response–related gene sets at age 30 months. *CYP19A1* mice showed a shift toward relative enrichment of epithelial-mesenchymal transition genes with age and duration of transgene expression.

Many Proliferation-Related Genes Identified as Significantly Differentially Expressed in *Esr1* Mice Are Found to Be Members of the Prosigna/PAM50 Breast Cancer Prognostic Panel

The Prosigna/PAM50 gene profile provides prognostic information about distant recurrence breast cancer patients with early-stage ER^+ cancer.[6] Of the 50 genes composing the profile, 25 of them were significantly differentially expressed at higher levels in the *Esr1* mice and 5 in the *CYP19A1* mice at age 24 months (Figure 5A). TPM values of representative proliferation- and estrogen-related genes were compared at the two age 24-month and one age 30-month end points, demonstrating that the lack of significant difference between the two genotypes in TPM values at the age 30-month end point was due to relative down-regulation of these genes at age 30 months in the *Esr1* mice (Figure 5B). Estrogen-regulated genes showed a different pattern between the two models (Figure 5C). Pituitary tumor-transforming gene 1 regulator of sister chromatid separation, securin (*Pttg1*) was expressed at significantly higher levels at both the age 24- and 30-month end points in *Esr1* mice. MYC proto-oncogene, basic helix-loop-helix transcription factor (*Myc*) and transmembrane protein 45B (*Tmem45b*) were expressed at significantly different levels only at the age 30-month end point, with *Myc* being expressed at higher levels in the *Esr1* mice and *Tmem45b* in the *CYP19A1* mice.

Significant Differentially Expressed Cell Proliferation–Related Genes Appear in the *Esr1* Mice within 1 Week of Transgene Induction

To test how long after transgene induction significant differences in cell proliferation and PAM50 prognostic panel-related genes appeared in the mice, RNAseq was performed on whole mammary gland tissue without palpable or visual tumor selected randomly before histologic analyses 1 week after transgene induction at ages 12 and 18 months. Transgene induction was confirmed at both ages in the *Esr1* and *CYP19A1* mice (Figure 6, A and B). At age 12 months, 1641 genes were expressed at significantly higher levels in *Esr1* and 1367 genes in *CYP19A1* mice (Figure 6C). Similar to results at age 24 months after 6 or 12 months of transgene induction, up-regulated genes in *Esr1* mice were significantly enriched in cell proliferation–related HALLMARK gene sets (HALLMARK_G2M_CHECKPOINT, HALLMARK_E2F TARGETS, and HALLMARK_MITOTIC SPINDLE) (Figure 6D). Enrichment in an immunologically related gene set, HALLMARK_ALLOGRAFT_REJECTION, was also found. Again, similar to results at age 24 months, up-regulated genes in *CYP19A1* mice were enriched in HALLMARK_MYOGENESIS and HALLMARK_ADIPOGENESIS (Figure 6E). A difference between the 24- and 12-month time points was the presence of significant enrichment in HALLMARK_ESTROGEN_RESPONSE gene sets in both *Esr1* and *CYP19A1* mice, albeit different genes in each genotype. At age 24 months, this was found only in the *Esr1* mice. At age 18 months, 1843 genes were expressed at significantly higher levels in *Esr1* and 1485 genes in *CYP19A1* mice (Figure 6F). HALLMARK_G2M_CHECKPOINT, HALLMARK_E2F TARGETS, and HALLMARK_MITOTIC SPINDLE were again the most significantly enriched gene sets in *Esr1* mice (Figure 6G). HALLMARK_MYOGENESIS was the most significantly enriched gene set in *CYP19A1* mice, similar to other time points (Figure 6H). Both genotypes showed enrichment of the HALLMARK_ESTROGEN_RESPONSE_LATE gene set at this time point, again by definition, the specific genes in the gene set being different between the two genotypes. Of the 50 genes in the Prosigna/PAM50 gene set, 23 were significantly differentially overexpressed in the *Esr1* compared with the *CYP19A1* mice 1 week following transgene induction, most at both 12 and 18 months of age (Figure 7A). Similarly, TPM expression values showed reproducible differences in relative expression levels of 15 identified ESTROGEN_RESPONSE_LATE genes between models across both the 12- and 18-month–old end points (Figure 7B).

Discussion

One significant aspect of the work is demonstrating that mouse models of the most common human breast cancer phenotype, ER^+ adenocarcinoma, are useful when mice are aged and carried through reproductive senescence. Because the study focused on conditional GEMM with overexpression of *Esr1* and *CYP19A1*, it does not answer whether additional GEMM might also exhibit a higher prevalence of high percentage ER^+ adenocarcinomas if they were similarly aged through reproductive senescence. However, this could be tested in future studies. Additional GEMMs exist that develop ER^+ mammary cancer, some that only exhibit this phenotype when they advance through reproductive senescence and are analyzed at ages beyond 20

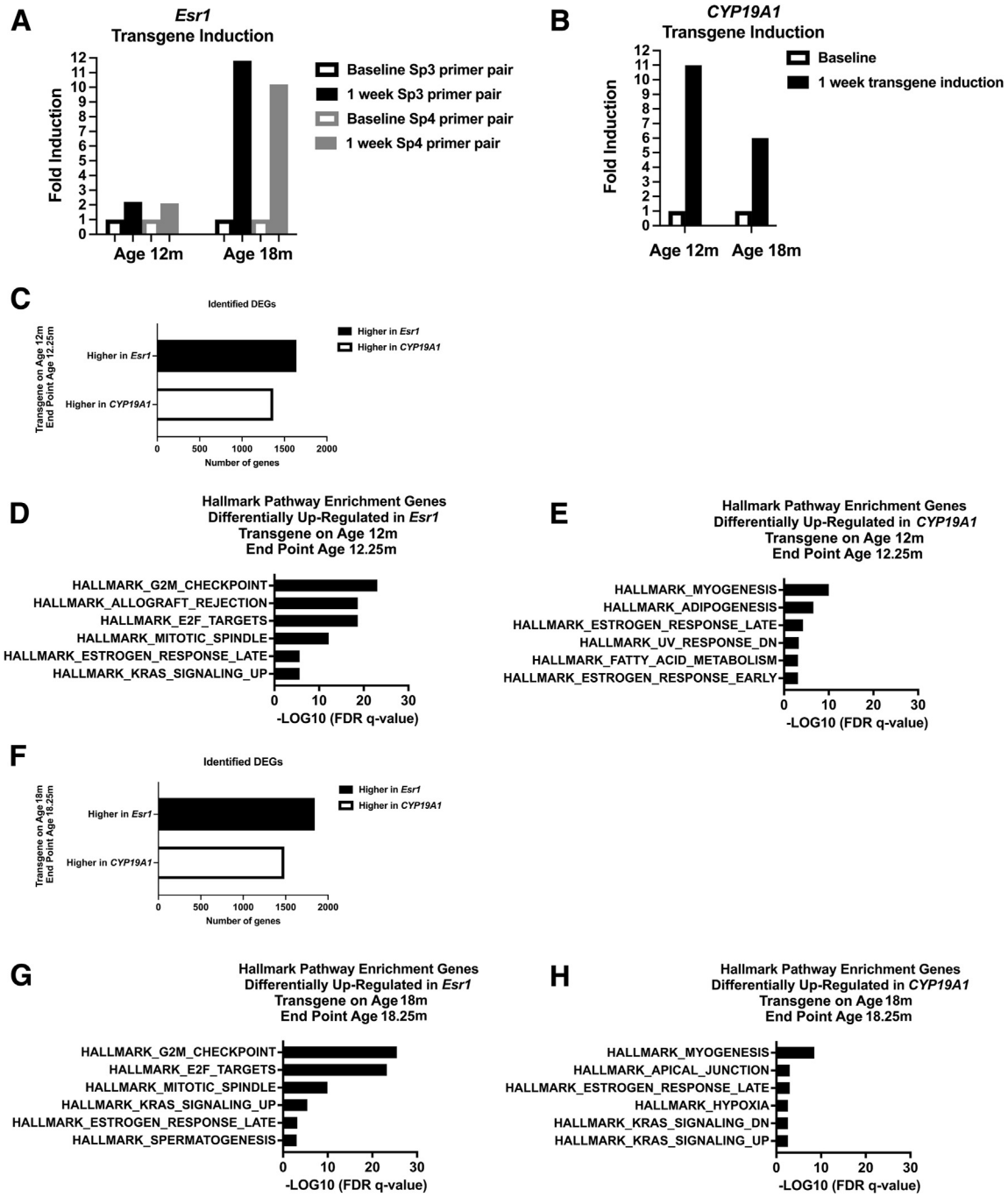

Figure 6 Significant differences in gene expression patterns appear within 1 week of transgene induction. **A:** Bar graph illustrates relative fold induction of mouse estrogen receptor 1 (estrogen receptor α; *Esr1*) transgene expression in mammary tissue at 1 week over baseline. Ages 12 and 18 months (m) shown. Results from two unique primer pairs (Sp3 and Sp4) shown. *Esr1*: Age 12m baseline $n = 1$. Age 12m 1 week: $n = 2$. Age 18m baseline $n = 2$. Age 18m 1 week: $n = 2$. **B:** Bar graph illustrates relative fold induction of human cytochrome P450 family 19 subfamily A member 1 (aromatase; *CYP19A1*) transgene expression in mammary tissue at 1 week over baseline. Ages 12 and 18m shown. *CYP19A1*: Age 12m baseline $n = 3$. Age 12m 1 week: $n = 4$. Age 18m baseline $n = 3$. Age 18m 1 week: $n = 3$. **C:** Bar graph presenting numbers of significantly differentially expressed genes (DEGs) in *Esr1* and *CYP19A1* mice within 1 week of transgene induction at age 12 months (adjusted $P < 0.05$, DESeq2). **D:** Bar graph presenting the six HALLMARK gene sets with the lowest significant false discovery rate (FDR) q-values identified from significant DEGs expressed at higher levels in *Esr1* mice with 1 week transgene induction at age 12m, end point age 12.25 months. **E:** Bar graph presenting the six HALLMARK gene sets with the lowest significant FDR q-values identified from significant DEGs expressed at higher levels in *CYP19A1* mice with 1 week transgene induction at age 12m, end point age 12.25 months. **F:** Bar graph presenting numbers of significant DEGs in *Esr1* and *CYP19A1* mice within 1 week of transgene induction at age 18 months (adjusted $P < 0.05$, DESeq2). **G:** Bar graph presenting the six HALLMARK gene sets with the lowest significant FDR q-values identified from significant DEGs expressed at higher levels in *Esr1* mice with 1 week transgene induction at age 18m, end point age 18.25 months. **H:** Bar graph presenting the six HALLMARK gene sets with the lowest significant FDR q-values identified from significant DEGs expressed at higher levels in *CYP19A1* mice with 1 week transgene induction at age 18m, end point age 18.25 months. Hallmark gene sets identified from Molecular Signatures Database version 7.5.1 (*http://www.gsea-msigdb.org/gsea/index.jsp*, last accessed June 21, 2022).

months.[41] A unique aspect of the conditional GEMM utilized herein is that they can be studied at younger and older ages, depending on when transgene expression is induced. In prior studies, appearance of preneoplasia and cancer was investigated in reproductive age *Esr1* and *CYP19A1* mice. Herein, similarities in phenotype were found independent of whether transgene expression was induced at age 12 or 18 months, but additional induction time points could be tested in future experiments.

Aging through reproductive senescence in mice is associated with appearance of mammary cancer, even in the absence of transgene expression, as exhibited by the 24-month−old mice in the absence of transgene induction. Any study examining mammary cancer generation in the presence of genetic manipulations needs to consider this background prevalence. In previous studies, *Esr1* mice have been shown to develop ER^+ adenocarcinomas before reproductive senescence; however, the appearance of cancers with high percentages of ER^+ cells has been limited to experiments where *Esr1* overexpression was combined with *Brca1* deletion with *Trp53* haploinsufficiency or Simian virus 40 T-antigen expression.[25,42] Mammary adenocarcinomas developing in reproductive age *CYP19A1* mice were generally defined as ER^-, in contrast to results found herein, where most adenocarcinomas found were ER^+ (with one exception).

The mechanism underlying the higher prevalence of ER^+ breast cancer in women after menopause is postulated to result from the higher numbers of proliferating ER^+ cells present in older compared with younger premenopausal women, possibly due to dysregulated *ESR1* expression.[2,3,43] Herein, it is possible that induction of *Esr1* expression in the GEMM collaborated with similar changes found commonly with age in mice to produce the higher prevalence of ER^+ cancer seen in the *Esr1* compared with *CYP19A1* mice. Although overexpression of both *Esr1* and *CYP19A1* lead to higher percentages of ER^+, progesterone receptor positive, and proliferating mammary epithelial cells,[15] at ages 12 and 18 months, *Esr1* transgene induction introduced significantly higher levels of several known estrogen response genes compared with *CYP19A1* mice. Analysis of significantly differentially expressed genes between the two models at age 24 months at both transgene induction times and at age 30 months revealed persistent significant enrichment of HALLMARK_ESTROGEN_RESPONSE_LATE genes.

Breast cancer is a highly prevalent cancer in women, but not all women develop clinically significant breast cancer during their lifetime, even if they age through their 90s.[44] It could be useful to develop prognostic tests for primary breast cancer appearance just as has been suggested for secondary breast cancer development and similar to what is currently being developed using polygenic risk scores.[8,18,45−47] If at least some transcriptional changes in a mouse model were to parallel changes found in women linked to higher risk of mammary cancer development, the mouse model could theoretically be used to help develop such a profile. To explore the possibility in the *Esr1* and *CYP19A1* mice, an established multigene prognostic profile developed for early-stage breast cancer, Prosigna/PAM50, was queried.[6,7] A profile employed for breast cancer prognostication was utilized because of the absence of clinically validated profiles for assessing primary breast cancer risk in women. Interestingly, numbers of genes that are members of the PAM50 profile were expressed at significantly higher levels in *Esr1* mice, whereas a small portion of genes contained within this profile were found expressed at significantly higher levels in the *CYP19A1* mice. Notably, significant differences in expression levels of these genes preceded cancer development. Most were identified as differentially expressed only 1 week after transgene expression at 12- and/or 18-month−old time points, consistent with the altered gene expression being mechanistically involved in cancer risk. Alternatively, the genes may only be markers of cancer risk, but either role would be relevant to their use in a profile for assessing the risk of breast cancer development.

In women and mice, mammary epithelial cell proliferation decreases with advancing age.[1,23] Herein, the *Esr1* mice demonstrated lower expression levels of cell proliferation−related genes that are members of the PAM50 gene profile at the age 30-month end point compared with the two 24-month end points. Representative examples include *Anln*, *Mki67*, and *Exo1*, biomarkers of prognosis with mechanistic links to breast cancer oncogenesis. Anillin is required for cytokinesis that, when knocked down in breast cancer cell lines, induces senescence.[48] Marker of proliferation Ki-67 is a well-established biomarker in breast cancer prognosis that can be linked to multiple steps of carcinogenesis from initiation through progression, metastases, and immune and drug responses.[49] Exonuclease 1 is a multifunction exonuclease belonging to the mismatch repair system.[50−52] It displays higher expression at early stages in breast as well as other cancers, and has genetic polymorphisms that are associated with varying levels of breast cancer risk. Estrogen-regulated genes are linked to breast carcinogenesis.[53] Three estrogen-regulated genes that are members of the PAM50 profile demonstrated significant differences in expression between the two models even at the age 30-month end point, 18 months after transgene induction. Pituitary tumor transforming gene (*PTTG*) 1 is an estrogen-regulated gene affecting cell cycle regulation, with higher levels correlating with decreased survival in breast cancer.[54] MYC proto-oncogene, BHLH transcription factor (*MYC*) is an estrogen-regulated gene that contributes to breast cancer genesis through multiple mechanisms.[55,56] *Tmem45b* was one of the few PAM50 genes significantly higher expressed in *CYP19A1* than in *Esr1* mice. It is an estrogen-regulated gene whose expression in cancer cells has been linked to changes in migration and invasion and is considered a prognostic biomarker for different cancer types.[57−59]

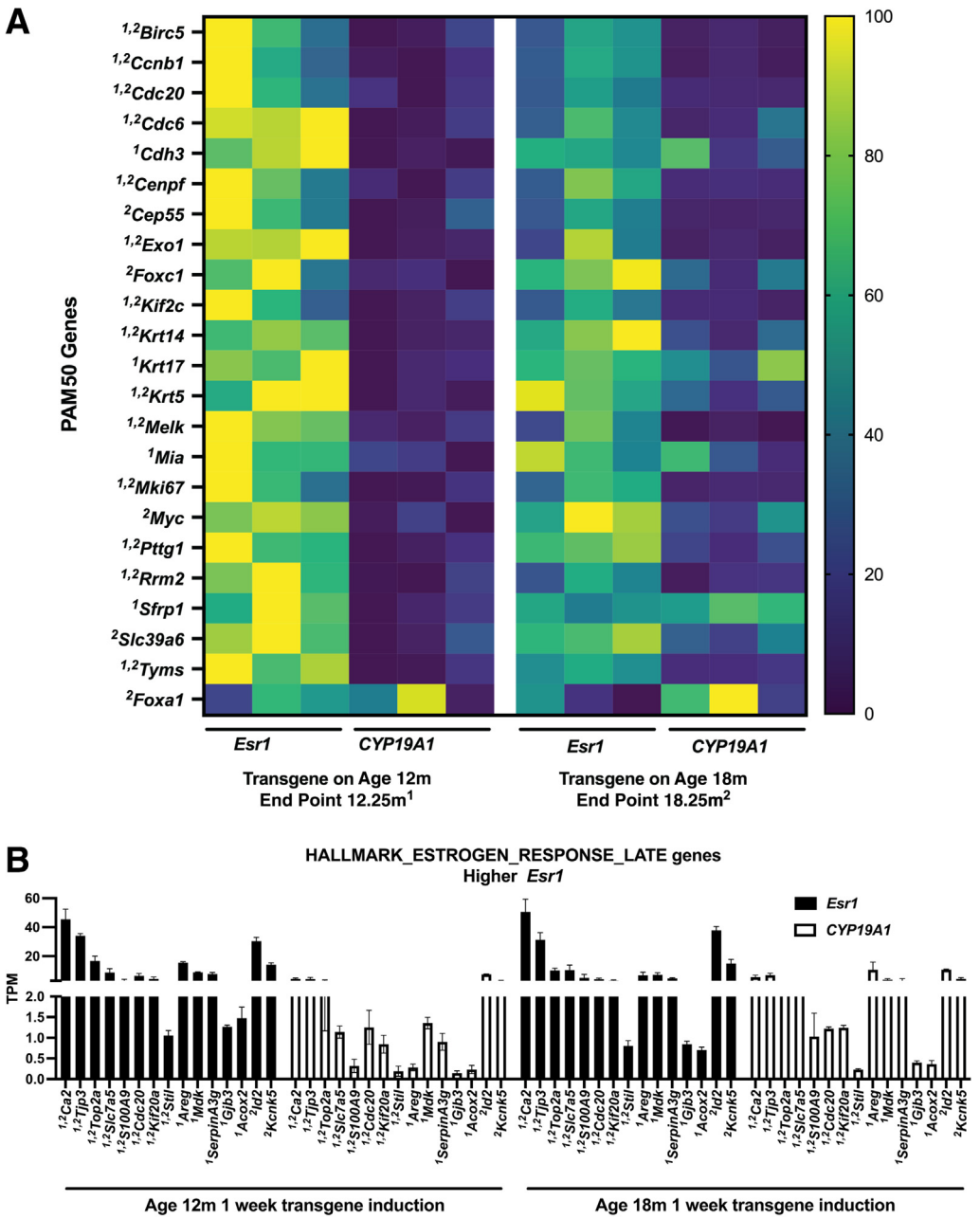

Figure 7 Elevated expression of cell proliferation genes linked to human prognostic profile appears within 1 week of mouse estrogen receptor 1 (estrogen receptor α; *Esr1*) transgene induction. **A:** Heat map comparing relative expression levels of differentially expressed genes (DEGs) that are members of the human estrogen receptor α—positive (ER$^+$)/HER2$^-$ breast cancer prognostic Prediction Analysis of Microarray (PAM) 50 profile in *Esr1* and human cytochrome P450 family 19 subfamily A member 1 (aromatase; *CYP19A1*) mice with transgene induction for 1 week at ages 12 and 18 months. Relative expression levels shown for unique individual samples ($n = 3$ for each cohort). Yellow indicates highest expression level, and dark blue indicates lowest expression level, for each gene. **B:** Bar graph illustrating transcripts per million (TPM) expression levels of 15 HALLMARK_ESTROGEN_RESPONSE_LATE genes expressed at significantly higher levels in *Esr1* compared with *CYP19A1* mice following 1 week transgene induction at 12 and/or 18 months of age (adjusted $P < 0.05$, DESeq2). 1: Adjusted $P < 0.05$, DESeq2, *Esr1* and *CYP19A1* mice, transgene induction at age 12m, end point age 12.25m. 2: Adjusted $P < 0.05$, DESeq2, *Esr1* and *CYP19A1* mice, transgene induction at age 18m, end point age 18.25 m. Data are given as means ± SEM (**B**). *Acox2*, acyl-coA oxidase 2; *Areg*, amphiregulin; *Birc5*, baculoviral IAP repeat containing 5; *Ca2*, carbonic anhydrase 2; *Ccnb1*, cyclin B1; *Cdc20*, cell division cycle 20; *Cdc6*, cell division cycle 6; *Cdh3*, cadherin 3; *Cenpf*, centromere protein F; *Cep55*, centrosomal protein 55; E2F, E2 transcription factor; *Exo1*, exonuclease 1; FDR, false discovery rate; *Foxa1*, forkhead box A1; *Foxc1*, forkhead box C1; G2M, G_2 phase; *Gjb3*, gap junction protein β 3; *Id2*, inhibitor of DNA binding 2; *Kcnk5*, potassium two pore domain channel subfamily K member 5; *Kif20a*, kinesin family member 20A; *Kif2c*, kinesin family member 2; KRAS, Kirsten rat sarcoma viral oncogene homolog; *Krt14*, keratin 14; *Krt17*, keratin 17; *Krt5*, keratin 5; *Mdk*, midkine; *Melk*, maternal embryonic leucine zipper kinase; *Mia*, MIA SH3 domain containing; *Mki67*, marker of proliferation Ki-67; *Myc*, MYC proto-oncogene, BHLH transcription factor; *Pttg1*, PTTG1 regulator of sister chromatid separation, securin; *Rrm2*, ribonucleotide reductase regulatory subunit M2; S100A9, S100 calcium binding protein A9; *SerpinA3g*, serine protease inhibitor A3G; *Sfrp1*, secreted frizzled-related protein 1; *Slc7a5*, solute carrier family 7 member 5; *Slc39a6*, solute carrier family 39 member 6; *Stil*, STIL centriolar assembly protein; *Tjp3*, tight junction protein 3; *Top2a*, DNA topoisomerase II α; *Tyms*, thymidylate synthetase.

Significant differences in expression levels of estrogen pathway genes were noted within 1 week of differential transgene expression. *Esr1* mice exhibited many more up-regulated estrogen pathway genes than *CYP19A1* mice. A high proportion of the genes identified as DEGs are known to be associated with breast cancer prognosis and/or pathways related to carcinogenesis, including differentiation and proliferation. Higher expression levels of carbonic anhydrase II, tight junction protein 3, cell division cycle 20, kinesin family member 20a, midkine, and gap junction protein β 3 in breast cancer have been linked to poor prognosis.[60–65] Stem cell leukemia/T-cell acute leukemia 1 interrupting locus centriolar assembly protein (STIL) is reported up-regulated in breast cancer, and in other cancer types it has been linked to poorer survival.[66] DNA topoisomerase II α and solute carrier family 7 member 5 are discussed as prognostic markers for evaluating the likelihood of invasive disease in patients with ductal carcinoma *in situ*.[67,68] S100 calcium binding protein a9 has been defined as a marker for precancerous apocrine lesions in the breast.[69] Increased acyl-CoA oxidase 2 expression level in ER^+ breast cancers is reported associated with a better prognosis.[70] Amphiregulin expression in ER^+ breast cancer shows significant age-dependent differences with younger (≤45 years) compared with older (≥70 years) patients showing higher expression.[71] Serpin family a member 3 is reported expressed in the murine mammary epithelial stem-like cell line, where it has been speculated it could prevent stem cells from differentiating.[72] Inhibitor of DNA binding 2 is considered a breast differentiation factor.[73] Potassium two pore domain channel subfamily K member 5 is an estrogen-regulated gene linked to estrogen-induced proliferation in breast cancer cells.[74]

In summary, the use of aged conditional GEMM with mammary epithelial cell-targeted *Esr1* and *CYP19A1* expression enabled the identification of several candidate genes that could be further investigated for use in human prognostic profiles for primary and secondary breast cancer development. The finding of a high proportion of ER^+ mammary cancers developing in these models with age past reproductive senescence supports the concept that age and changes in reproductive hormone levels contribute to breast cancer phenotype, specifically the higher prevalence of ER^+ breast cancers in aging women. Demonstration of a higher risk of mammary cancer development with *Esr1* compared with *CYP19A1* overexpression illustrates the significance of estrogen receptor α in breast cancer risk. The development of models and experimental paradigms for studying ER^+ mammary cancer in mice will contribute to further investigation of genetic risk profiles, preventive interventions, and how mechanisms of aging influence cancer risk.

Acknowledgments

We thank Georgetown University–Lombardi Shared Resources Animal Models, Genomics and Epigenomics, Histopathology and Tissue for contributions to the research; and Vipa Patel for assisting in the preliminary statistical analyses of oocyte counts.

Author Contributions

P.A.F. conceived the study; P.A.F., W.W., and J.A.F. designed the study; P.A.F., W.W., K.K., B.L.R., V.M., J.W., X.Z., and J.A.F. acquired data; P.A.F., K.K., B.L.R., G.K., V.M., C.S., and J.A.F. analyzed data; P.A.F. and B.L.R. wrote the initial manuscript; P.A.F., W.W., K.K., B.L.R., G.K., V.M., C.S., J.W., X.Z., and J.A.F. reviewed the final manuscript; and P.A.F. secured funding. P.A.F. is the guarantor of this work and, as such, had full access to all of the data in the study and takes responsibility for the integrity of the data and the accuracy of the data analysis.

Supplemental Data

Supplemental material for this article can be found at *http://doi.org/10.1016/j.ajpath.2022.09.008*.

References

1. Benz CC: Impact of aging on the biology of breast cancer. Crit Rev Oncol Hematol 2008, 66:65–74
2. Walker RA, Martin CV: The aged breast. J Pathol 2007, 211: 232–240
3. Porras L, Ismail H, Mader S: Positive regulation of estrogen receptor alpha in breast tumorigenesis. Cells 2021, 10:2966
4. McNamara KM, Sasano H: The intracrinology of breast cancer. J Steroid Biochem Mol Biol 2015, 145:172–178
5. Lim VW, Li J, Gong Y, Jin A, Yuan J-M, Yong EL, Koh W-P: Serum estrogen receptor bioactivity and breast cancer risk among postmenopausal women. Endocr Relat Cancer 2014, 21:263–273
6. Vieira AF, Schmitt F: An update on breast cancer multigene prognostic tests—emergent clinical biomarkers. Front Med (Lausanne) 2018, 5:248
7. Gordon-Craig S, Parks RM, Cheung K-L: The potential use of tumour-based prognostic and predictive tools in older women with primary breast cancer: a narrative review. Oncol Ther 2020, 8: 231–250
8. Alothman SJ, Kang K, Liu X, Krawczyk E, Azhar RI, Hu R, Goerlitz D, Kallakury BV, Furth PA: Characterization of transcriptome diversity and in vitro behavior of primary human high-risk breast cells. Sci Rep 2022, 12:6159
9. Abdi E, Latifi-Navid S, Latifi-Navid H: LncRNA polymorphisms and breast cancer risk. Pathol Res Pract 2022, 229:153729
10. Slepicka PF, Somasundara AVH, dos Santos CO: The molecular basis of mammary gland development and epithelial differentiation. Semin Cell Dev Biol 2021, 114:93–112
11. Mori H, Cardiff RD, Borowsky AD: Aging mouse models reveal complex tumor-microenvironment interactions in cancer progression. Front Cell Dev Biol 2018, 6:35
12. Holen I, Speirs V, Morrissey B, Blyth K: In vivo models in breast cancer research: progress, challenges and future directions. Dis Models Mech 2017, 10:359–371
13. Frech MS, Halama ED, Tilli MT, Singh B, Gunther EJ, Chodosh LA, Flaws JA, Furth PA: Deregulated estrogen receptor alpha expression in mammary epithelial cells of transgenic mice results in the development of ductal carcinoma in situ. Cancer Res 2005, 65:681–685

14. Miermont AM, Cabrera MC, Frech SM, Nakles RE, Diaz-Cruz ES, Shiffert MT, Furth PA: Association of over-expressed estrogen receptor alpha with development of tamoxifen resistant hyperplasia and adenocarcinomas in genetically engineered mice. Anat Physiol 2012, Suppl 12:001
15. Díaz-Cruz ES, Sugimoto Y, Gallicano GI, Brueggemeier RW, Furth PA: Comparison of increased aromatase versus ER[alpha] in the generation of mammary hyperplasia and cancer. Cancer Res 2011, 71:5477−5487
16. Dabydeen SA, Kang K, Díaz-Cruz ES, Alamri A, Axelrod ML, Bouker KB, Al-Kharboosh R, Clarke R, Hennighausen L, Furth PA: Comparison of tamoxifen and letrozole response in mammary preneoplasia of ER and aromatase overexpressing mice defines an immune-associated gene signature linked to tamoxifen resistance. Carcinogenesis 2015, 36:122−132
17. Pardo I, Lillemoe HA, Blosser RJ, Choi M, Sauder CAM, Doxey DK, Mathieson T, Hancock BA, Baptiste D, Atale R, Hickenbotham M, Zhu J, Glasscock J, Storniolo AMV, Zheng F, Doerge R, Liu Y, Badve S, Radovich M, Clare SE: Next-generation transcriptome sequencing of the premenopausal breast epithelium using specimens from a normal human breast tissue bank. Breast Cancer Res 2014, 16:R26
18. Bodelon C, Oh H, Derkach A, Sampson JN, Sprague BL, Vacek P, Weaver DL, Fan S, Palakal M, Papathomas D, Xiang J, Patel DA, Linville L, Clare SE, Visscher DW, Mies C, Hewitt SM, Brinton LA, Storniolo AMV, He C, Chanock SJ, Garcia-Closas M, Gierach GL, Figueroa JD: Polygenic risk score for the prediction of breast cancer is related to lesser terminal duct lobular unit involution of the breast. npj Breast Cancer 2020, 6:41
19. Palliyaguru DL, Vieira Ligo Teixeira C, Duregon E, di Germanio C, Alfaras I, Mitchell SJ, Navas-Enamorado I, Shiroma EJ, Studenski S, Bernier M, Camandola S, Price NL, Ferrucci L, de Cabo R; SLAM Investigators: Study of Longitudinal Aging in Mice: presentation of experimental techniques. J Gerontol A Biol Sci Med Sci 2021, 76: 552−560
20. Ackert-Bicknell CL, Anderson LC, Sheehan S, Hill WG, Chang B, Churchill GA, Chesler EJ, Korstanje R, Peters LL: Aging research using mouse models. Curr Proto Mouse Biol 2015, 5:95−133
21. Wilkinson MJ, Selman C, McLaughlin L, Horan L, Hamilton L, Gilbert C, Chadwick C, Flynn JN: Progressing the care, husbandry and management of ageing mice used in scientific studies. Lab Anim 2020, 54:225−238
22. Jackson SJ, Andrews N, Ball D, Bellantuono I, Gray J, Hachoumi L, Holmes A, Latcham J, Petrie A, Potter P, Rice A, Ritchie A, Stewart M, Strepka C, Yeoman M, Chapman K: Does age matter? the impact of rodent age on study outcomes. Lab Anim 2017, 51:160−169
23. Raafat A, Strizzi L, Lashin K, Ginsburg E, McCurdy D, Salomon D, Smith GH, Medina D, Callahan R: Effects of age and parity on mammary gland lesions and progenitor cells in the FVB/N-RC mice. PLoS One 2012, 7:e43624
24. Miermont AM, Parrish AR, Furth PA: Role of ER[alpha] in the differential response of Stat5a loss in susceptibility to mammary preneoplasia and DMBA-induced carcinogenesis. Carcinogenesis 2010, 31:1124−1131
25. Jones LP, Tilli MT, Assefnia S, Torre K, Halama ED, Parrish A, Rosen EM, Furth PA: Activation of estrogen signaling pathways collaborates with loss of Brca1 to promote development of ER [alpha]-negative and ER[alpha]-positive mammary preneoplasia and cancer. Oncogene 2008, 27:794−802
26. Nakles RE, Shiffert MT, Díaz-Cruz ES, Cabrera MC, Alotaiby M, Miermont AM, Riegel AT, Furth PA: Altered AIB1 or AIB1Δ3 expression impacts ER[alpha] effects on mammary gland stromal and epithelial content. Mol Endocrinol 2011, 25:549−563
27. Frech MS, Torre KM, Robinson GW, Furth PA: Loss of cyclin D1 in concert with deregulated estrogen receptor alpha expression induces DNA damage response activation and interrupts mammary gland morphogenesis. Oncogene 2008, 27:3186−3193
28. Hruska KS, Tilli MT, Ren S, Cotarla I, Kwong T, Li M, Fondell JD, Hewitt JA, Koos RD, Furth PA, Flaws JA: Conditional overexpression of estrogen receptor alpha in a transgenic mouse model. Transgenic Res 2002, 11:361−372
29. Li M, Hu J, Heermeier K, Hennighausen L, Furth PA: Apoptosis and remodeling of mammary gland tissue during involution proceeds through p53-independent pathways. Cell Growth Differ 1996, 7: 13−20
30. Alothman SJ, Wang W, Goerlitz DS, Islam M, Zhong X, Kishore A, Azhar RI, Kallakury BV, Furth PA: Responsiveness of Brca1 and Trp53 deficiency−induced mammary preneoplasia to selective estrogen modulators versus an aromatase inhibitor in Mus musculus. Cancer Prev Res 2017, 10:244−254
31. Medina D: Premalignant and malignant mammary lesions induced by MMTV and chemical carcinogens. J Mammary Gland Biol Neoplasia 2008, 13:271−277
32. Dobin A, Davis CA, Schlesinger F, Drenkow J, Zaleski C, Jha S, Batut P, Chaisson M, Gingeras TR: STAR: ultrafast universal RNA-seq aligner. Bioinformatics 2013, 29:15−21
33. Risso D, Ngai J, Speed TP, Dudoit S: Normalization of RNA-seq data using factor analysis of control genes or samples. Nat Biotechnol 2014, 32:896−902
34. Li B, Dewey CN: RSEM: accurate transcript quantification from RNA-Seq data with or without a reference genome. BMC Bioinformatics 2011, 12:323
35. Love MI, Huber W, Anders S: Moderated estimation of fold change and dispersion for RNA-seq data with DESeq2. Genome Biol 2014, 15:550
36. Subramanian A, Tamayo P, Mootha VK, Mukherjee S, Ebert BL, Gillette MA, Paulovich A, Pomeroy SL, Golub TR, Lander ES, Mesirov JP: Gene set enrichment analysis: a knowledge-based approach for interpreting genome-wide expression profiles. Proc Natl Acad Sci U S A 2005, 102:15545−15550
37. Liberzon A, Birger C, Thorvaldsdóttir H, Ghandi M, Mesirov JP, Tamayo P: The Molecular Signatures Database (MSigDB) hallmark gene set collection. Cell Syst 2015, 1:417−425
38. Edgar R, Domrachev M, Lash AE: Gene Expression Omnibus: NCBI gene expression and hybridization array data repository. Nucleic Acids Res 2002, 30:207−210
39. Gonsioroski A, Meling DD, Gao L, Plewa MJ, Flaws JA: Iodoacetic acid affects estrous cyclicity, ovarian gene expression, and hormone levels in mice. Biol Reprod 2021, 105:1030−1042
40. Rattan S, Brehm E, Gao L, Niermann S, Flaws JA: Prenatal exposure to di(2-ethylhexyl) phthalate disrupts ovarian function in a transgenerational manner in female mice. Biol Reprod 2018, 98:130−145
41. Dabydeen SA, Furth PA: Genetically engineered ER[alpha]-positive breast cancer mouse models. Endocr Relat Cancer 2014, 21: R195−R208
42. Tilli MT, Frech MS, Steed ME, Hruska KS, Johnson MD, Flaws JA, Furth PA: Introduction of estrogen receptor-[alpha] into the tTA/TAg conditional mouse model precipitates the development of estrogen-responsive mammary adenocarcinoma. Am J Pathol 2003, 163: 1713−1719
43. Quong J, Eppenberger-Castori S, Moore D, Scott GK, Birrer MJ, Kueng W, Eppenberger U, Benz CC: Age-dependent changes in breast cancer hormone receptors and oxidant stress markers. Breast Cancer Res Treat 2002, 76:221−236
44. Neves D, Souza J, Chagas S: Breast cancer in nonagenarians: single institutional experience in development country. J Clin Oncol 2018, 36:e22032
45. Shrestha A, Cullinane C, Evoy D, Geraghty J, Rothwell J, Walshe J, McCartan D, McDermott E, Prichard R: Clinical treatment score post-5 years as a predictor of late distant recurrence in hormone receptor-positive breast cancer: systematic review and meta-analysis. Br J Surg 2022, 109:411−417
46. Pedersen RN, Esen BÖ, Mellemkjær L, Christiansen P, Ejlertsen B, Lash TL, Nørgaard M, Cronin-Fenton D: The incidence of breast

cancer recurrence 10-32 years after primary diagnosis. J Natl Cancer Inst 2021, 114:391−399
47. Behravan H, Hartikainen JM, Tengström M, Kosma V-M, Mannermaa A: Predicting breast cancer risk using interacting genetic and demographic factors and machine learning. Sci Rep 2020, 10: 11044
48. Magnusson K, Gremel G, Rydén L, Pontén V, Uhlén M, Dimberg A, Jirström K, Pontén F: ANLN is a prognostic biomarker independent of Ki-67 and essential for cell cycle progression in primary breast cancer. BMC Cancer 2016, 16:904
49. Mrouj K, Andrés-Sánchez N, Dubra G, Singh P, Sobecki M, Chahar D, Al Ghoul E, Aznar AB, Prieto S, Pirot N, Bernex F, Bordignon B, Hassen-Khodja C, Villalba M, Krasinska L, Fisher D: Ki-67 regulates global gene expression and promotes sequential stages of carcinogenesis. Proc Natl Acad Sci U S A 2021, 118. e2026507118
50. Wang H-C, Chiu C-F, Tsai R-Y, Kuo Y-S, Chen H-S, Wang R-F, Tsai C-W, Chang C-H, Lin C-C, Bau D-T: Association of genetic polymorphisms of EXO1 gene with risk of breast cancer in Taiwan. Anticancer Res 2009, 29:3897−3901
51. Yan S, Gao S, Zhou P: Multi-functions of exonuclease 1 in DNA damage response and cancer susceptibility. Radiat Med Prot 2021, 2: 146−154
52. Chic N, Schettini F, Brasó-Maristany F, Sanfeliu E, Adamo B, Vidal M, Martínez D, Galván P, González-Farré B, Cortés J, Gavilá J, Saura C, Oliveira M, Pernas S, Martínez-Sáez O, Soberino J, Ciruelos E, Carey LA, Muñoz M, Perou CM, Pascual T, Bellet M, Prat A: Oestrogen receptor activity in hormone-dependent breast cancer during chemotherapy. EBioMedicine 2021, 69:103451
53. Ikeda K, Horie-Inoue K, Inoue S: Identification of estrogen-responsive genes based on the DNA binding properties of estrogen receptors using high-throughput sequencing technology. Acta Pharmacol Sin 2015, 36:24−31
54. Meng C, Zou Y, Hong W, Bao C, Jia X: Estrogen-regulated PTTG1 promotes breast cancer progression by regulating cyclin kinase expression. Mol Med 2020, 26:33
55. Xu J, Chen Y, Olopade OI: MYC and breast cancer. Genes Cancer 2010, 1:629−640
56. Shang Y, Hu X, DiRenzo J, Lazar MA, Brown M: Cofactor dynamics and sufficiency in estrogen receptor−regulated transcription. Cell 2000, 103:843−852
57. Kaczynski P, Bauersachs S, Baryla M, Goryszewska E, Muszak J, Grzegorzewski WJ, Waclawik A: Estradiol-17[beta]-induced changes in the porcine endometrial transcriptome in vivo. Int J Mol Sci 2020, 21:890
58. Schmit K, Michiels C: TMEM proteins in cancer: a review. Front Pharmacol 2018, 9:1345
59. Shen K, Yu W, Yu Y, Liu X, Cui X: Knockdown of TMEM45B inhibits cell proliferation and invasion in gastric cancer. Biomed Pharmacother 2018, 104:576−581
60. Mboge MY, Mahon BP, McKenna R, Frost SC: Carbonic anhydrases: role in pH control and cancer. Metabolites 2018, 8:19
61. Martin TA, Watkins G, Mansel RE, Jiang WG: Loss of tight junction plaque molecules in breast cancer tissues is associated with a poor prognosis in patients with breast cancer. Eur J Cancer 2004, 40: 2717−2725
62. Karra H, Repo H, Ahonen I, Löyttyniemi E, Pitkänen R, Lintunen M, Kuopio T, Söderström M, Kronqvist P: Cdc20 and securin overexpression predict short-term breast cancer survival. Br J Cancer 2014, 110:2905−2913
63. Li T-F, Zeng H-J, Shan Z, Ye R-Y, Cheang T-Y, Zhang Y-J, Lu S-H, Zhang Q, Shao N, Lin Y: Overexpression of kinesin superfamily members as prognostic biomarkers of breast cancer. Cancer Cell Int 2020, 20:123
64. Li F, Tian P, Zhang J, Kou C: The clinical and prognostic significance of midkine in breast cancer patients. Tumor Biol 2015, 36: 9789−9794
65. Liu S, Song A, Zhou X, Huo Z, Yao S, Yang B, Liu Y, Wang Y: ceRNA network development and tumour-infiltrating immune cell analysis of metastatic breast cancer to bone. J Bone Oncol 2020, 24: 100304
66. Li J, Yang Z, Qi Y, Liu X, Liu Y, Gao X, Li S, Zhu J, Zhang C, Du E, Zhang Z: STIL acts as an oncogenetic driver in a primary cilia-dependent manner in human cancer. Front Cell Dev Biol 2022, 10: 804419
67. Buckley N, Boyle D, McArt D, Irwin G, Harkin DP, Lioe T, McQuaid S, James JA, Maxwell P, Hamilton P, Mullan PB, Salto-Tellez M: Molecular classification of non-invasive breast lesions for personalised therapy and chemoprevention. Oncotarget 2015, 6: 43244−43254
68. Badve SS, Cho S, Gökmen-Polar Y, Sui Y, Chadwick C, McDonough E, Sood A, Taylor M, Zavodszky M, Tan PH, Gerdes M, Harris AL, Ginty F: Multi-protein spatial signatures in ductal carcinoma in situ (DCIS) of breast. Br J Cancer 2021, 124:1150−1159
69. Celis JE, Moreira JMA, Gromova I, Cabezón T, Gromov P, Shen T, Timmermans V, Rank F: Characterization of breast precancerous lesions and myoepithelial hyperplasia in sclerosing adenosis with apocrine metaplasia. Mol Oncol 2007, 1:97−119
70. Bjørklund SS, Kristensen VN, Seiler M, Kumar S, Alnæs GIG, Ming Y, Kerrigan J, Naume B, Sachidanandam R, Bhanot G, Børresen-Dale A-L, Ganesan S: Expression of an estrogen-regulated variant transcript of the peroxisomal branched chain fatty acid oxidase ACOX2 in breast carcinomas. BMC Cancer 2015, 15:524
71. Yau C, Fedele V, Roydasgupta R, Fridlyand J, Hubbard A, Gray JW, Chew K, Dairkee SH, Moore DH, Schittulli F, Tommasi S, Paradiso A, Albertson DG, Benz CC: Aging impacts transcriptomes but not genomes of hormone-dependent breast cancers. Breast Cancer Res 2007, 9:R59
72. Williams C, Helguero L, Edvardsson K, Haldosén L-A, Gustafsson J-Å: Gene expression in murine mammary epithelial stem cell-like cells shows similarities to human breast cancer gene expression. Breast Cancer Res 2009, 11:R26
73. Candia P de, Benera R, Solit DB: A role for Id proteins in mammary gland physiology and tumorigenesis. Adv Cancer Res 2004, 92:81−94
74. Alvarez-Baron CP, Jonsson P, Thomas C, Dryer SE, Williams C: The two-pore domain potassium channel KCNK5: induction by estrogen receptor [alpha] and role in proliferation of breast cancer cells. Mol Endocrinol 2011, 25:1326−1336